Heliyon 10 (2024) e34135

Contents lists available at ScienceDirect

Heliyon

journal homepage: www.cell.com/heliyon

Research article

Exploring the antidiabetic and anti-inflammatory potential of *Lavandula officinalis* essential oil: *In vitro* and *in silico* insights

Hamza Assaggaf [a,1], Naoufal El Hachlafi [b,c,1], Amine Elbouzidi [d], Mohamed Taibi [d,e], Sulaiman Mohammed Alnasser [f], Hajar Bendaif [g], Youssra Aalilou [c], Ahmed Qasem [a], Ammar Attar [a], Abdelhakim Bouyahya [h,**], Chrismawan Ardianto [i,*], Long Chiau Ming [i,j,k], Khang Wen Goh [l], Kawtar Fikri-Benbrahim [b], Hanae Naceiri Mrabti [m,n]

[a] *Department of Laboratory Medicine, Faculty of Applied Medical Sciences, Umm Al-Qura University, Makkah, 21955, Saudi Arabia*
[b] *Laboratory of Microbial Biotechnology and Bioactive Molecules, Faculty of Sciences and Technologies Faculty, Sidi Mohamed Ben Abdellah University, P.O. Box 2202, Imouzzer Road, Fez, Morocco*
[c] *Laboratories of Pharmacology and Toxicology, Pharmaceutical and Toxicological Analysis Research Team, Faculty of Medicine and Pharmacy, Mohammed V University in Rabat, Rabat, Morocco*
[d] *Laboratoire d'Amélioration des Productions Agricoles, Biotechnologie et Environnement (LAPABE), Faculté des Sciences, Morocco des Sciences, Université Mohammed Premier, Oujda, 60000, Morocco*
[e] *Centre de l'Oriental des Sciences et Technologies de l'Eau et de l'Environnement (COSTEE), Université Mohammed Premier, Oujda, 60000, Morocco*
[f] *Department of Pharmacology and Toxicology, College of Pharmacy, Qassim University, Qassim, 51452, Saudi Arabia*
[g] *Laboratoire des Ressources Naturelles et Environnement, Faculté Polydisciplinaire de Taza, Morocco*
[h] *Laboratory of Human Pathologies Biology, Faculty of Sciences, Mohammed V University in Rabat, Rabat, 10106, Morocco*
[i] *Department of Pharmacy Practice, Faculty of Pharmacy, Universitas Airlangga, Surabaya, Indonesia*
[j] *School of Medical and Life Sciences, Sunway University, Sunway City, 47500, Malaysia*
[k] *Pengiran Anak Puteri Rashidah Sa'adatul Bolkiah Institute of Health Sciences, Universiti Brunei Darussalam, Gadong, BE1410, Brunei Darussalam*
[l] *Faculty of Data Science and Information Technology, INTI International University, Nilai, Malaysia*
[m] *High Institute of Nursing Professions and Health Techniques Casablanca, Casablanca, 20250, Morocco*
[n] *Euromed Research Center, Euromed Faculty of Pharmacy, School of Engineering and Biotechnology, Euromed University of Fes (UEMF), Meknes Road, Fez, 30000, Morocco*

ARTICLE INFO

Keywords:
α-Amylase
α-Glucosidase
Anti-inflammatory activity
Lipoxygenase
Anti-tyrosinase
ADMET analysis
Molecular docking
Human and health

ABSTRACT

Medicinal plants have been utilized for centuries in traditional medicine systems worldwide, providing a rich source of bioactive compounds with diverse biological activities. *Lavandula officinalis*, a member of the Lamiaceae family, has been recognized for its multifaceted pharmacological activities. In this current investigation, our primary objective was to scrutinize the *in vitro* inhibitory potential of *L. officinalis* essential oil (LOEO) against alpha-amylase and alpha-glucosidase, with the aim of understanding its antidiabetic effects. Additionally, the assay encompassed tyrosinase and lipoxygenase (LOX) to assess its anti-inflammatory attributes. Unraveling the underlying molecular mechanisms of these activities prompted an *in-silico* study. The purpose was to establish correlations between *in-vitro* observations and computational

* Corresponding author.
** Corresponding author.
E-mail addresses: a.bouyahya@um5r.ac.ma (A. Bouyahya), chrismawan-a@ff.unair.ac.id (C. Ardianto).
[1] Co-first authors

https://doi.org/10.1016/j.heliyon.2024.e34135
Received 23 February 2024; Received in revised form 29 April 2024; Accepted 3 July 2024
Available online 5 July 2024

Diabetes
Cardiovascular disease

insights derived from molecular docking, which forecasts the interaction of LOEO molecules with their respective targets, alongside ADMET prediction. The Gas Chromatography-Mass Spectrometry (GC-MS) analysis allow to identify eighteen compounds, with the dominance of L−camphor (43.12 %), 1,8−cineole (34.27 %) and borneol (8.60 %) in LOEO. The antidiabetic evaluation revealed that LOEO exhibited noteworthy inhibitory activity against both α-amylase and α-glucosidase, displaying IC_{50} values of 3.14 ± 0.05 mg/mL and 2.07 ± 0.03 mg/mL, respectively. The subsequent *in-silico* study highlighted the particularly strong binding affinity of (E)-Farnesene, with a binding score of −7.4 kcal/mol for alpha-glucosidase, while Germacrene D displayed the highest affinity among the ligands (−7.9 kcal/mol) for the alpha-amylase target. Furthermore, the investigation into *in vitro* anti-inflammatory activity unveiled LOEO efficacy against tyrosinase (IC_{50} = 42.74 μg/mL) and LOX (IC_{50} = 11.58 ± 0.07 μg/mL). The *in-silico* analysis echoed these findings, indicating α-Cadinene's notable binding affinity of 6 kcal/mol with tyrosinase and α-Cedrene's binding score of −6.5 kcal/mol for LOX. Impressively, for both COX-1 and COX-2, α-Cedrene exhibited significant binding affinities of −7.6 and −7.3 kcal/mol, respectively. The convergence between the *in vitro* and *in silico* outcomes underscores the potential of LOEO and its constituent compounds as potent inhibitors targeting both diabetes and the inflammatory processes.

1. Introduction

Diabetes mellitus (DM) stands as a multifaceted and complicated metabolic disorder that exerts influence over the intricate glucose regulation within the human physiological framework. This disorder is narrowly defined by the presence of elevated blood glucose levels, or hyperglycemia. It segregates into two primary pathogenetic classifications: type 1 (T1D) and type 2 (T2D). Among these, T2D prevails as the most prevalent manifestation, accounting for approximately 90–95 % of diagnosed instances [1]. An array of suppositions has arisen to elucidate the involved mechanisms underpinning the genesis of diabetes, striving to identify established risk factors. These encompass unhealthy behaviors typified by a Western lifestyle, characterized by sedentary habits and inadequate physical exertion, culminating in excess weight gain and predisposition to obesity [1,2]. Multiple avenues of investigation have unveiled the interplay between obesity and insulin resistance, ultimately paving the path to diabetes [1–3]. Concurrently, a range of studies proffer the assertion that inflammatory pathways serve as pivotal pathogenetic agents in the natural course of diabetes. Concurrently, a range of studies proffer the assertion that inflammatory pathways serve as pivotal pathogenetic agents in the natural course of diabetes. Numerous research endeavors strive to target these inflammatory pathways as key constituents in strategies for preventing or managing diabetes and its associated complications. Notably, certain agents that regulate glucose levels, such as glitazones or statins, alongside high-dose insulin, have demonstrated potential to mitigate inflammatory markers [1,4]. Piperazine ferulate emerges as a promising therapeutic agent in diabetic nephropathy, offering renal protection through modulation of endothelial nitric oxide synthase [5]. In the context of these multifaceted considerations, recent studies shed light on various therapeutic strategies addressing diabetes-associated health conditions. Mendelian randomization studies delineate positive causal links between T2D and a spectrum of ocular diseases, highlighting the need for comprehensive management approaches [6]. Innovations in insulin delivery methods, encompassing diverse administration routes, herald a personalized approach to diabetes management in younger populations [7]. Furthermore, emerging research underscores the potential of exosomal circular RNA in enhancing diabetic foot ulcer wound healing, providing novel insights into therapeutic interventions for this debilitating complication [8]. These findings collectively underscore the imperative for tailored therapeutic interventions and ongoing research endeavors to unravel the intricate mechanisms underlying diabetes-associated health conditions, thereby advancing personalized care and improving patient outcomes.

Within this context, the quest for novel molecular candidates remains paramount, drawing upon the wellspring of natural biodiversity and its reservoir of bioactive compounds. Aromatic and medicinal plants, exemplified by *Lavandula officinalis* (also known as *Lavandula angustifolia*), emerge as a copious source of essential oils, renowned across epochs for their diverse pharmacological properties that enrich the therapeutic armamentarium. *L. officinalis*, hailing from the Lamiaceae family and specifically the Lavandula genus, encompassing 28 species, has exhibited a native presence spanning the Cape, Canary Islands, Madeira, Europe, the Mediterranean Basin, Asia, and Southwest Asia to Southeast India [9]. This botanical entity has enjoyed historical employment in traditional medicine to address nervous disorders, and contemporary investigations have delved into its neuroprotective and psychotropic attributes [10–13].

Furthermore, *L. officinalis* has unveiled an array of pharmacological virtues, including antioxidative activity [9,14,15], antimicrobial efficacy [2,14–19], antiviral capabilities [20], anti-inflammatory attributes [15,21,22], along with antiapoptotic, anticancer, dermatoprotective, and analgesic properties [13–15,21,23,24]. Additionally, it has demonstrated potential as an antihyperglycemic agent [25].

This present study's primary objective revolves around the revelation of LOEO chemical composition via gas chromatography-mass spectrometry (GC/MS). The overarching aim is to explore the principal chemical constituents of LOEO in the context of anti-inflammatory and antidiabetic activities, targeting key enzymes. A comprehensive analysis spanning *in vitro* and *in silico* realms has been conducted to unveil the underlying mechanisms operating within this dual pathway network. It is noteworthy that, to the best of our knowledge, no prior research has explored the *in vitro* antidiabetic attributes of LOEO or delved into the pivotal enzymes underpinning anti-inflammatory effects, rendering our investigation the inaugural endeavor in this domain.

2. Materials and methods

2.1. Plant material and EO extraction

The leaves of *L. officinalis* were harvested from its natural habitat in Taza region, Morocco (34° 13′ 00″ N, 4° 01′ 00″ W, March 2022) at blooming period May 2022. The plant was identified according to the procedure established by González-Tejero et al. [26], and accomplished by the botanist Pr. Amina Bari from department of Biology, University Sidi Mohamed Ben Abdallah, Fez, and deposited under voucher specimens BLMUP 401 at the laboratory of Microbial biotechnology. The aerial parts were dried under specific circumstances (at 25 °C and continuous aeriation, at dark place) and the EOs were obtained via hydrodistillation, using a Clevenger-type device for 180 min. Then, the oil was recovered and dehydrated with Na_2SO_4 and placed at 4 °C until upcoming assays.

2.2. GC-MS analysis

Phytochemical analysis of LOEO were determined with a Hewlett–Packard Gas Chromatographer HP 6890 coupled with a mass spectrometer (MS) HP5973 model, and equipped with an HP-5MS (5 % phenylmethyl siloxane) capillary column (30 m × 0.25 mm × film thickness 0.25 μm) as described in the literature [27,28]. The run started initially with a temperature of 45 °C for 2 min then increased gradually to 300 °C. The temperature of the injector was kept at 250 °C whereas the detector's temperature was held at 280 °C. Automatic sample injection was applied (1 μL, split ratio of 1:15) and the carrier gas used was Helium with a flow rate of 1.41 mL/min. The following conditions were applied for the mass spectrometry: the temperature of the ion source was set at 200 °C, an ionization voltage of 70 eV, and the scan range was performed from 35 to 500 amu. The individual GC peaks' mass spectra were identified using a computer search of the commercial libraries (WILEY, NIST). The identification was validated by comparison with published data and by calculating the retention indices (RI) in relation to (C_8–C_{24}) n-alkanes 17. Peak area percentage was used for quantification, and the results were presented as the average of three measurements. The concentration ranges of the identified compounds were around 0.06 % and 43.12 %.

2.3. PASS, ADME, the prediction of the toxicity analysis (Pro−Tox II)

To predict the pharmacological activity of the main chemical constituents of LOEO, we have utilized the PASS method, a computational tool used for predicting the biological activity of chemical compounds [29,30]. It uses a statistical algorithm to compare the chemical structure of a compound with a large database of known bioactive compounds, and predicts the likelihood of the compound exhibiting certain activities, such as binding to specific receptors, inhibiting enzymes, or affecting metabolic pathways. First, the chemical compounds were transformed into SMILES format through ChemDraw and then analyzed using the PASS online program, which indicated the probable activity (Pa) and likely inactivity (Pi) of the drug−like compounds. Absorption, Distribution, Metabolism, and Excretion are key factors that determine the pharmacokinetic profile of a compound, or how it is absorbed, distributed, metabolized, and eliminated from the body. Computational tools are used to predict the ADME properties of compounds, such as their permeability across cell membranes, their affinity for transporters and enzymes involved in drug absorption and elimination, and their metabolic stability [29]. For this reason, we assessed the physicochemical properties, drug similarity, and pharmacokinetic properties of the compounds using ADME webservers such as SwissADME (http://www.swissadme.ch/accessed on July 20, 2023) [31], and pkCSM (http://biosig.unimelb.edu.au/pkcsm/accessed on July 20, 2023) [32].

To estimate toxicity levels, the Pro−Tox II online tool (https://tox−new.charite.de/protox II/accessed on July 20, 2023) was used [33–35]. This online tool uses a statistical algorithm to compare the chemical structure of a compound with a large database of known

Table 1
Molecular modeling proteins and grid−box parameters.

Proteins	PDB ID	Grid Box Size	Grid Box Center	Native Ligand	Reference
Lipoxygenase	1N8Q	size_x = 40 size_y = 40 size_z = 40	center_x = 22.455 center_y = 1.293 center_z = 20.362	Protocatechuic acid	[39]
Tyrosinase	5I3B	size_x = 40 size_y = 40 size_z = 40	center_x = 17.728 center_y = 96.86 center_z = 32.239	Hydroquinone	[40]
Human COX−2	5IKV	size_x = 40 size_y = 40 size_z = 40	center_x = 159.311 center_y = 199.702 center_z = 208.426	Flufenamic acid	[41]
Ovine COX−1	5WBE	size_x = 40 size_y = 40 size_z = 40	center_x = 27.478 center_y = 156.699 center_z = 4.873	Mofezolac	[42]
α−Glucosidase	5NN5	size_x = 40 size_y = 40 size_z = 40	center_x = 1.591 center_y = −26.552 center_z = 87.364	Acarbose	[44]
α−amylase	1SMD	size_x = 40 size_y = 40 size_z = 40	center_x = 8.349 center_y = 58.705 center_z = 19.096	Acarbose	[43]

toxic compounds, and predicts the likelihood of the compound causing toxicity or adverse effects in humans or other organisms. This tool provided information on the LD_{50} values, toxicity class, and the toxicological endpoints, including hepatotoxicity, carcinogenicity, immunotoxicity, mutagenicity, and cytotoxicity.

2.4. Molecular docking protocol

The molecular docking analysis was performed as described in References [36–38]. Protein structures of four anti−inflammatory target proteins, lipoxygenase (LOX, PDB ID: 1N8Q) [39], tyrosinase (PDB ID: 5I3B) [40], human COX−2 (PDB: 5IKV) [41], and ovine COX−1 (PDB: 5WBE) [42], and two anti-diabetes-involved proteins α−amylase (PDB ID: 1SMD) [43], and α−Glucosidase (PDB ID: 5NN5) [44] (Table 1). The protein structures were acquired from the Protein Data Bank https://www.rcsb.org/structure accessed on July 25, 2023, in a crystallographic 3D structure and adopted as docking targets, using Autodock Tools (version 1.5.6). The protein structures were stripped of H_2O molecules, metal atoms, co−crystalized ligands, and other non−covalently bound substances. Following the addition of Kollman charges, polar hydrogens and the merge of nonpolar hydrogens, the target file was saved as an appropriate pdbqt format. Ligands identified in LOEO were constructed as follows: sdf (3D conformer) file was downloaded from PubChem (https://pubchem.ncbi.nlm.nih.gov/) (accessed on July 25, 2023) and then converted to a pdb file by using PyMol. The ligand final pdbqt file was obtained by using Autodock Tools (version 1.5.6). Rigid molecular docking was executed with Autodock Vina's embedded scoring function [45]. The grid box representing the docking search space was resized to best match the active binding site. Table 8 shows the grid box coordinates. The docked ligand complexes' data were given as ΔG binding energy values (kcal/mol). Discovery Studio 4.1 (Dassault Systems Biovia, San Diego, CA, USA) was used to examine protein–ligand binding interactions and in the construction of 2D schemes of molecular interactions.

2.5. Biological activities

2.5.1. α−Amylase and α−glucosidase inhibitory activities

These tests aimed to assess the ability of LOEO to inhibit enzymes involved in carbohydrate metabolism (α−amylase and α−glucosidase), focusing on its anti−diabetic potential. The results obtained from these tests may provide information on the potential use of LOEO as a natural remedy for managing blood sugar levels in cases of diabetes or pre−diabetes.

i. α−Amylase Inhibitory Assay

For the α−amylase assay, 250 μL of LOEO was mixed with 250 μL of 0.02 M sodium phosphate buffer (pH = 6.9) containing α−amylase at a concentration of 240 U/mL. The mixture was incubated for 20 min at 37 °C. Next, 250 μL of 1 % starch solution prepared in 0.02 M sodium phosphate buffer (pH = 6.9) was added, followed by a further 15−minute incubation at 37 °C to allow the enzyme−substrate reaction. After this, 1 mL DNS (3,5−dinitrosalicylic acid) was added to stop the enzymatic reaction, and the mixture was incubated in a boiling water bath for 10 min. Once cooled, the reaction mixture was diluted by adding 2 mL of distilled water, and absorbance was measured at 540 nm using a spectrophotometer. The inhibitory effect of HE on α−amylase was expressed as percentage inhibition, the acquired data were then expressed as the half inhibitory concentration (IC_{50}) through three independent experimental runs (n = 3). Acarbose, a known α−amylase inhibitor, was used as a positive control (0.062, 0.12, 0.25, 0.5 and 1 mg/mL).

ii. α−Glucosidase Inhibitory Assay

For the α−glucosidase assay, 200 μL of LOEO was mixed with 100 μL of 0.1 M sodium phosphate buffer (pH = 6.7) containing the α−glucosidase enzyme solution at a concentration of 0.1 U/mL. The mixture was pre−incubated at 37 °C for 10 min. After this pre−incubation, 200 μL of 1 mM pNPG (p−nitrophenyl−α−D−glucopyranoside) solution in 0.1 M sodium phosphate buffer (pH = 6.7) was added to the mixture. The mixture was then incubated at 37 °C for 30 min to allow the enzyme−substrate reaction. After incubation, 1 mL of 0.1 M Na_2CO_3 was added to stop the enzymatic reaction, and absorbance was recorded at 405 nm using a spectrophotometer. The inhibitory effect of LOEO on α−glucosidase was expressed as percentage inhibition, and the acquired data were then expressed as the IC_{50} through three independent experimental runs (n = 3). Acarbose, a known α−glucosidase inhibitor, was used as a positive control (0.062, 0.12, 0.25, 0.5 and 1 mg/mL).

2.5.2. Anti-inflammatory assays

i. Lipoxygenase Inhibition

The assessment of the *in vitro* anti-inflammatory potential of LOEO involved the evaluation of its inhibitory activity against 5-Lipoxygenase (5-LOX), as per the methodology previously published [46]. In a succinct overview, 20 μL of Essential Oils (EOs) and 20 μL of 5-LOX derived from Glycine max (at a concentration of 100 U/mL) were subjected to pre-incubation with 200 μL of a phosphate buffer (0.1 M, pH 9) at ambient temperature for a duration of 5 min. Subsequently, 20 μL of linolenic acid (at a concentration of 4.18 mM in ethanol) was introduced to initiate the enzymatic reaction, which was meticulously monitored for a duration of 3 min at a wavelength of 234 nm. The acquired data were then expressed as the IC_{50} through three independent experimental runs (n = 3).

2.5.3. In vitro anti-tyrosinase

The evaluation of the dermatoprotective potential of LOEO included an assessment of its tyrosinase inhibitory activity, employing a method previously outlined [47], with minor modifications. Succinctly, a volume of 20 μL of LOEO was introduced to a solution comprising 0.1 mL of tyrosinase (at a concentration of 333 U/mL) and 50 mM phosphate buffer at pH 6.5. This mixture was then maintained at a temperature of 37 °C for a duration of 10 min. Subsequently, 0.3 mL of L-DOPA substrates (at a concentration of 5 mM) were introduced. Following an incubation period of 30–40 min at 37 °C, the absorbance was measured at 510 nm using a UV–Vis 1240 spectrophotometer. The acquired data were then expressed as IC_{50} through three independent experimental runs (n = 3). Quercetin was utilized as a standard reference in this context.

2.6. Statistical analysis

The results were presented as the average value ± the standard deviation, calculated from three independent experimental runs for each measurement. To assess differences in the observed parameters among the samples, we employed analysis of variance (ANOVA). All statistical data processing was conducted using the SPSS software package.

3. Results and discussion

3.1. Phytochemical analysis using GC−MS

Essential oils are complex mixtures of volatile and non−volatile molecules, typically consisting of numerous compounds in varying proportions, and they exhibit diverse chemical structures and functions. The specific chemical composition of these oils can be influenced by various factors, such as the plant's developmental stage, the harvested organs, the time of harvest, and the geographical location [48–52]. In the case of LOEO, its chemical composition and the percentage of each identified compound, along with retention index (RI) values, are provided in Table 2. Gas chromatography−mass spectrometry (GC−MS) analysis revealed the presence of eighteen volatile compounds, accounting for 99.68 % of the total oil. The major constituents in LOEO are oxygenated monoterpenes (86.63 %), with L−camphor (43.12 %), 1,8−cineole (34.27 %), Borneol (8.60 %), and Carvone (5.65 %) being the predominant compounds (Fig. 1).

Numerous scientific studies have investigated the chemical composition of LOEO from different regions worldwide. A recently published work on LOEO from Eastern Morocco, indicated the predominance of linalool, accounting for 14.93 % of the composition. Other notable constituents included camphor at 14.11 %, linalyl acetate at 11.17 %, and eucalyptol at 10.99 % [53]. Previous investigations have unveiled variations in the qualitative and quantitative makeup of EOs from different regions within Morocco. For instance, in the Rabat Sale-Zemour-Zaers region, previous studies have reported linalool (44.67 %), linalyl acetate (42 %), 1.8-cineole (5.30 %), and camphor (6.02 %) as the principal compounds [13,54]. Meanwhile, in Azrou, situated in the Middle Moroccan Atlas, a study conducted by Tablaoui et al., revealed that linalyl acetate (44.96 %) and linalool (44.64 %) were the major components in LOEO [55]. Interestingly, a separate Moroccan study yielded different outcomes, with linalool (21.81 %), 1,8-cineole (18.07 %), camphor

Table 2
Phytochemical profile of the LOEO.

N°	Compounds	RI	% Area
1	Camphene	951	0.45
2	β−Pinene	974	0.32
3	1,8−cineole	1046	**34.27**
4	γ−Terpinene	1017	0.26
5	L−camphor	1143	**43.12**
6	Borneol	1169	8.60
7	1,3,8−*p*−Menthatriene	1457	0.59
8	Carvone	1240	5.65
9	(−)−Bornyl acetate	1289	1.62
10	Allyl Tiglate	1370	1.05
11	Cuminaldehyde	1240	1.56
12	Trans−Ocimene	1032	0.28
13	*(E)*−Farnesene	1449	0.29
14	α−Cedrene	1458	0.49
15	(Z)− Trans− α−Bergamotene	1496	0.38
16	(−)−β−Funebrene	1415	0.06
17	α−Cadinene	1532	2.04
18	Germacrene D	1563	0.66
	Monoterpene hydrocarbons (%)		1.89
	Oxygenated monoterpenes (%)		86.63
	Sesquiterpene hydrocarbons (%)		3.92
	Oxygenated sesquiterpenes (%)		4.57
	Others (%)		2.67
	Total identified compounds %		**99.68**

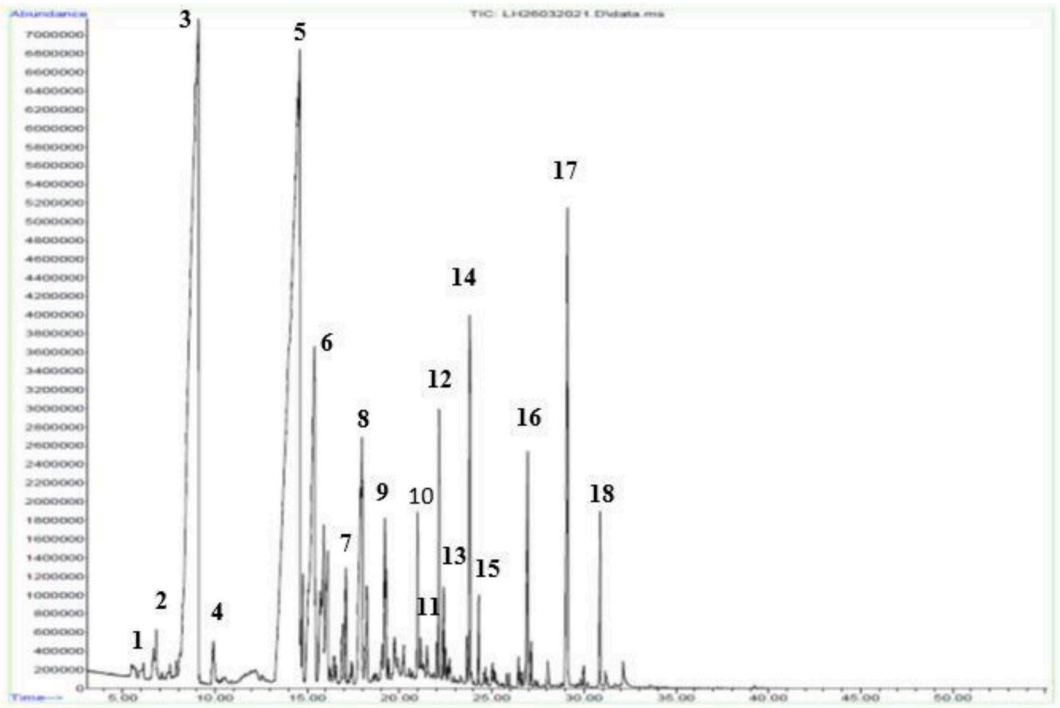

Fig. 1. GC–MS chromatogram of the composition of LOEO. Note: the corresponding molecules are in Table 2.

(11.89 %), and linalyl acetate (10.21 %) as the primary components [56].

For instance, Chahboun et *al.* [57], analyzed the LOEO obtained from flowers grown in Morocco, identifying 53 terpene compounds, with 3–Benzylsulfonyl–2, 6,6–trimethylbicyclo (3.1.1) heptane (23.61 %), Linalyl phenyl acetate (15.98 %), Campholen aldehyd (9.17 %), Borneol (9.3 %), Eucalyptol (7.77 %), and gamma Caldinen (11.64 %) as major components.

Similarly, Verma et *al.* [58], examined the composition of *L. officinalis* flowers from Uttarakand, India, identifying 37 monoterpene compounds with linalyl acetate (47.56 %), Linalool (28.06 %), lavandulyl acetate (4.34 %), and α–terpineol (3.7 %) as the primary constituents. Meanwhile, Kulevanova et *al.* [59], studied the LOEO flowers collected from the mountain of Kozjak, Macedonia, detecting 32 constituents with a dominance of Linalool (25.7 %), linalyl acetate (23.2 %), and lavandulyl acetate (12.4 %), along with

Table 3
Physiochemical and drug–likeness analysis of the major compounds found in LOEO**. (1)** Camphene, **(2)** β–Pinene, **(3)** 1,8–cineole, **(4)** γ–Terpinene, **(5)** L–camphor, **(6)** Borneol, **(7)** 1,3,8–*p*–Menthatriene, **(8)** Carvone, **(9)** (–)–Bornyl acetate, **(10)** Allyl Tiglate, **(11)** Cuminaldehyde, **(12)** *trans*–Ocimene, **(13)** *(E)*–Farnesene, **(14)** α–Cedrene, **(15)** *(Z)*–*trans*– α–Bergamotene, **(16)** (–)–β–Funebrene, **(17)** α–Cadinene, **(18)** Germacrene D.

N°	HBD	HBA	TPSA (Å^2)	Log Po/w (WLOGP)	Log S (SILICO S–IT)	Lipinski's Rule of Five	Veber filter
1	0	0	0.00	3.00	3.08 (+++)	Yes; 0 violation	Yes; 0 violation
2	0	0	0.00	3.00	3.08 (+++)	Yes; 0 violation	Yes; 0 violation
3	0	1	9.23	2.74	2.86 (+++)	Yes; 0 violation	Yes; 0 violation
4	0	0	0.00	3.31	2.95	Yes; 0 violation	Yes; 0 violation
5	0	1	17.07	2.40	2.85	Yes; 0 violation	Yes; 0 violation
6	1	1	20.23	2.19	2.27	Yes; 0 violation	Yes; 0 violation
7	0	0	0.00	3.23	2.96	Yes; 0 violation	Yes; 0 violation
8	0	1	17.07	2.49	2.64	Yes; 0 violation	Yes; 0 violation
9	0	2	26.30	2.76	2.66	Yes; 0 violation	Yes; 0 violation
10	0	2	26.30	1.68	1.58	Yes; 0 violation	Yes; 0 violation
11	0	1	17.07	2.62	2.96	Yes; 0 violation	Yes; 0 violation
12	0	0	0.00	3.48	2.88	Yes; 0 violation	Yes; 0 violation
13	0	0	0.00	5.20	4.76	Yes; 0 violation	Yes; 0 violation
14	0	0	0.00	4.42	3.91	Yes; 1 violation: MLOGP>4.15	Yes; 0 violation
15	0	0	0.00	4.73	4.27	Yes; 1 violation: MLOGP>4.15	Yes; 0 violation
16	0	0	0.00	4.42	4.19	Yes; 1 violation: MLOGP>4.15	Yes; 0 violation
17	0	0	0.00	4.58	3.73	Yes; 1 violation: MLOGP>4.15	Yes; 0 violation
18	0	0	0.00	4.89	4.01	Yes; 1 violation: MLOGP>4.15	Yes; 0 violation

HBD: Hydrogen–Bond Donors; **HBA:** Hydrogen–Bond Acceptors; **Log Po/w:** distribution coefficient P; **Log S:** Solubility; (+++) Soluble.

Table 4
The (ADME) pharmacokinetic characteristics of the identified compounds present in LOEO. **(1)** Camphene, **(2)** β−Pinene, **(3)** 1,8−cineole, **(4)** γ−Terpinene, **(5)** L−camphor, **(6)** Borneol, **(7)** 1,3,8−*p*−Menthatriene, **(8)** Carvone, **(9)** (−)−Bornyl acetate, **(10)** Allyl Tiglate, **(11)** Cuminaldehyde, **(12)** *trans*−Ocimene, **(13)** *(E)*−Farnesene, **(14)** α−Cedrene, **(15)** *(Z)*−*trans*− α−Bergamotene, **(16)** (−)−β−Funebrene, **(17)** α−Cadinene, **(18)** Germacrene D.

Prediction	1	2	3	4	5	6	7	8	9	10	11	12	13	14	15	16	17	18
ADME Prediction																		
Absorption Parameters																		
Bioavailability score	0.55	0.55	0.55	0.55	0.55	0.55	0.55	0.55	0.55	0.55	0.55	0.55	0.55	0.55	0.55	0.55	0.55	0.55
Caco−2 Permeability	1.387	1.385	1.485	1.414	1.499	1.484	1.402	1.413	1.855	1.429	1.609	1.406	1.412	1.403	1.395	1.397	1.415	1.436
Intestinal Absorption (%)	94.14	95.52	96.50	96.21	95.96	93.43	96.04	97.70	95.36	97.30	95.84	94.72	93.46	96.57	96.22	95.24	94.64	95.59
Distribution Parameters																		
Log K_p (cm/s)	−1.435	−1.653	−2.437	−1.489	−2.002	−2.174	−1.732	−2.145	−2.233	−2.276	−1.196	−1.065	−1.217	−1.792	−1.677	−2.088	−1.443	−1.429
VDss	0.547	0.685	0.491	0.412	0.331	0.337	0.392	0.179	0.307	−0.087	0.324	0.336	0.547	0.774	0.861	0.680	0.678	0.544
BBB Permeability	0.787	0.818	0.368	0.754	0.612	0.646	0.735	0.588	0.553	0.392	0.438	0.761	0.815	0.811	0.860	0.853	0.785	0.723
Metabolism Parameters																		
CYP2D6, and CYP3A4 Substrate	No	No	No	No	No	No	No	No	No	No	No	No	No	No	No	No	No	No
CYP2D6, and CYP3A4 Inhibitors	No	No	No	No	No	No	No	No	No	No	No	No	No	No	No	No	No	No
Excretion Parameters																		
Total Clearance	0.049	0.03	1.009	0.217	0.109	1.035	0.253	0.225	1.029	0.987	0.227	0.441	1.810	0.929	1.176	0.941	1.18	1.42
Renal OCT2 Substrate	No	No	No	No	No	No	No	No	No	No	No	No	No	No	No	No	No	No

BBB: blood−brain barrier; Log BB > 0.3, molecule BBB permeant, Log BB < −1 molecule poorly distributed across the BBB.

the presence of sesquiterpene hydrocarbons and their oxygenated derivatives. These studies collectively demonstrate that LOEO cultivated in different regions across the globe tends to exhibit a predominance of monoterpene compounds, albeit with varying contents in each case.

These findings collectively underscore the substantial genetic diversity within Moroccan lavender species, which likely contributes to the observed variations in EO compositions. Furthermore, it is essential to consider the potential influence of varying climatic conditions across these distinct regions on EO composition [51].

The absence of linalool among the main constituents of LOEO in our study highlights the complexity of abiotic factors that can influence the chemical composition of plants. This absence could be the result of several such factors, including climatic variations, soil quality, altitude and exposure to sunlight. Previous studies have shown that these environmental conditions can affect the biosynthesis of volatile compounds in plants, leading to variations in their chemical composition [28,60,61].

3.2. Physiochemical and pharmacokinetic properties (ADME) of LOEO

Table 3 displays the physiochemical and drug−likeness analysis of major compounds obtained from lavender essential oil (LOEO). The analysis includes parameters such as Hydrogen−Bond Donors (HBD), Hydrogen−Bond Acceptors (HBA), Topological Polar Surface Area (TPSA), distribution coefficient (Log Po/w), and solubility (Log S). Additionally, the Lipinski's Rule of Five and Veber filter were applied to assess drug−likeness. The analysis highlights significant drug−likeness features among the compounds. Compounds 1 and 2 (Camphene and β−Pinene) show no hydrogen−bond donors or acceptors, low Total Polar Surface Area (TPSA), and a moderate distribution coefficient P (Log Po/w). Their high solubility (Log S) and adherence to Lipinski's Rule of Five and Veber filter criteria make them promising drug−like candidates. Compound 3 (1,8−cineole) possesses one hydrogen−bond acceptor, a relatively larger TPSA, and a lower Log Po/w value, further supporting its drug−like potential. Compounds 4, 7, and 12 (γ−Terpinene, 1,3,8−*p*−Menthatriene, and *trans*−Ocimene) lack hydrogen−bond donors or acceptors, resulting in higher Log Po/w values and lower solubility, yet they still comply with Lipinski's Rule of Five and Veber filter. Compounds 5, 8, and 11 (L−camphor, Carvone, and Cuminaldehyde) exhibit one hydrogen−bond acceptor, a relatively larger TPSA, and moderate Log Po/w values, demonstrating promise in terms of drug−likeness according to Lipinski's Rule of Five and Veber filter. Compound 6 (Borneol) stands out with one hydrogen−bond donor and acceptor, a larger TPSA, and lower Log Po/w value, making it moderately soluble and drug−like as per Lipinski's Rule of Five and Veber filter. Compounds 9 and 10 ((−)−Bornyl acetate and Allyl Tiglate) have two hydrogen−bond acceptors, leading to larger TPSA values. Although their distribution coefficient P values affect solubility, they still satisfy Lipinski's Rule of Five and Veber filter. Compounds 13 to 18 ((E)−Farnesene, α−Cedrene, (Z)−*trans*−α−Bergamotene, (−)−β−Funebrene, α−Cadinene, and Germacrene D) lack hydrogen−bond donors or acceptors, resulting in no TPSA. Despite their higher Log Po/w values and lower solubility, they still pass the Veber filter despite violating Lipinski's Rule of Five.

The results suggest that these compounds have potential therapeutic applications due to their physiochemical properties and adherence to drug−likeness criteria. Nonetheless, additional *in vitro* and *in vivo* investigations are imperative to verify their effectiveness and safety.

In this research study, we investigated the ADME (Absorption, Distribution, Metabolism, and Excretion) pharmacokinetic characteristics of major compounds found in LOEO (Table 4). The parameters are categorized into four groups: absorption parameters, distribution parameters, metabolism parameters, and excretion parameters. The bioavailability score, predicts the fraction of an orally administered compound that reaches systemic circulation. The bioavailability score ranges from 0 to 1, and a score closer to 1 indicates better bioavailability [62]. Looking at the Absorption Parameters, we find three key metrics: Bioavailability score, Caco−2 Permeability, and Intestinal Absorption (%). The bioavailability score ranges from 0 to 1 and reflects the fraction of the administered dose that can reach the bloodstream unchanged. All compounds exhibited a consistent bioavailability score of 0.55, indicating moderate bioavailability, making these compounds more readily accessible for therapeutic effects. Caco−2 Permeability, predicts the intestinal permeability of a compound using the Caco−2 cell model [63], the Caco−2 permeability values ranged from 1.385 to 1.855, suggesting good permeability for most compounds. Moreover, the intestinal absorption percentages were high, ranging from 93.43 % to 97.70 %.

A compound is considered to have a relatively low skin permeability if its Log Kp value is greater than −2.5. A Log Kp (cm/s) value above −2.5 indicates that the compound is less likely to efficiently permeate the skin barrier, making it less readily absorbed through the skin. In contrast, compounds with Log Kp values below −2.5 are considered to have higher skin permeability, as they can more easily penetrate the skin and be absorbed into the systemic circulation. For most compounds, Log Kp values are around −2.7, indicating limited distribution. None of LOEO's compounds have a Log Kp > -2.5 value, which indicates that these compounds have a poor skin permeability. The VDss values varied from 0.179 to 0.861, representing the volume of distribution at steady−state. The values vary between 0.179 and 0.861, reflecting the distribution of compounds in the body. Higher values suggest a higher volume of distribution. The BBB Permeability assesses the ability of the compounds to cross the blood−brain barrier. A Log BB value higher than 0.3 indicates blood−brain barrier (BBB) permeability. Interestingly, all LOEO compounds possess a Log BB greater than 0.3, demonstrating their capacity to cross the BBB.

To anticipate the potential drug metabolism or toxicity of a molecule, it is crucial to assess its predicted activity and interactions with cytochrome P450 (CYP) isozymes. The activity of a molecule pertains to its effects on biological systems, such as its ability to bind to specific receptors or enzymes. Understanding how a molecule interacts with CYP isozymes, which play a vital role in metabolizing numerous drugs, can provide valuable insights into its pharmacokinetic properties [64]. Notably, all identified compounds in LOEO are neither substrates nor inhibitors of the cytochrome P450 (CYP) enzymes CYP2D6 and CYP3A4, which are essential in drug metabolism [64]. Furthermore, none of the compounds have been found to be substrates of the Renal Organic Cation Transporter 2

(OCT2), responsible for eliminating various drugs through the kidneys [65]. Efficient renal clearance, facilitated by major organic cation transporters like Renal OCT2, is critical for drug metabolism.

To determine the total clearance of the compounds, both hepatic and renal clearance were assessed [32]. The total clearance values ranged from 0.03 to 1.810, signifying different rates of elimination for each compound. These pharmacokinetic considerations will play a pivotal role in evaluating the compounds' suitability for potential therapeutic applications and understanding potential health implications associated with the consumption of LOEO.

In order to evaluate the likelihood of the identified phytoconstituents being absorbed orally, we analyzed six key physicochemical properties: lipophilicity, size, polarity, solubility, flexibility, and saturation. These attributes play pivotal roles in determining a molecule's capacity to be absorbed and utilized within the body. To visually represent this information, we employed bioavailability radars, as shown in Fig. 2, which demonstrate the potential oral bioavailability of the compounds.

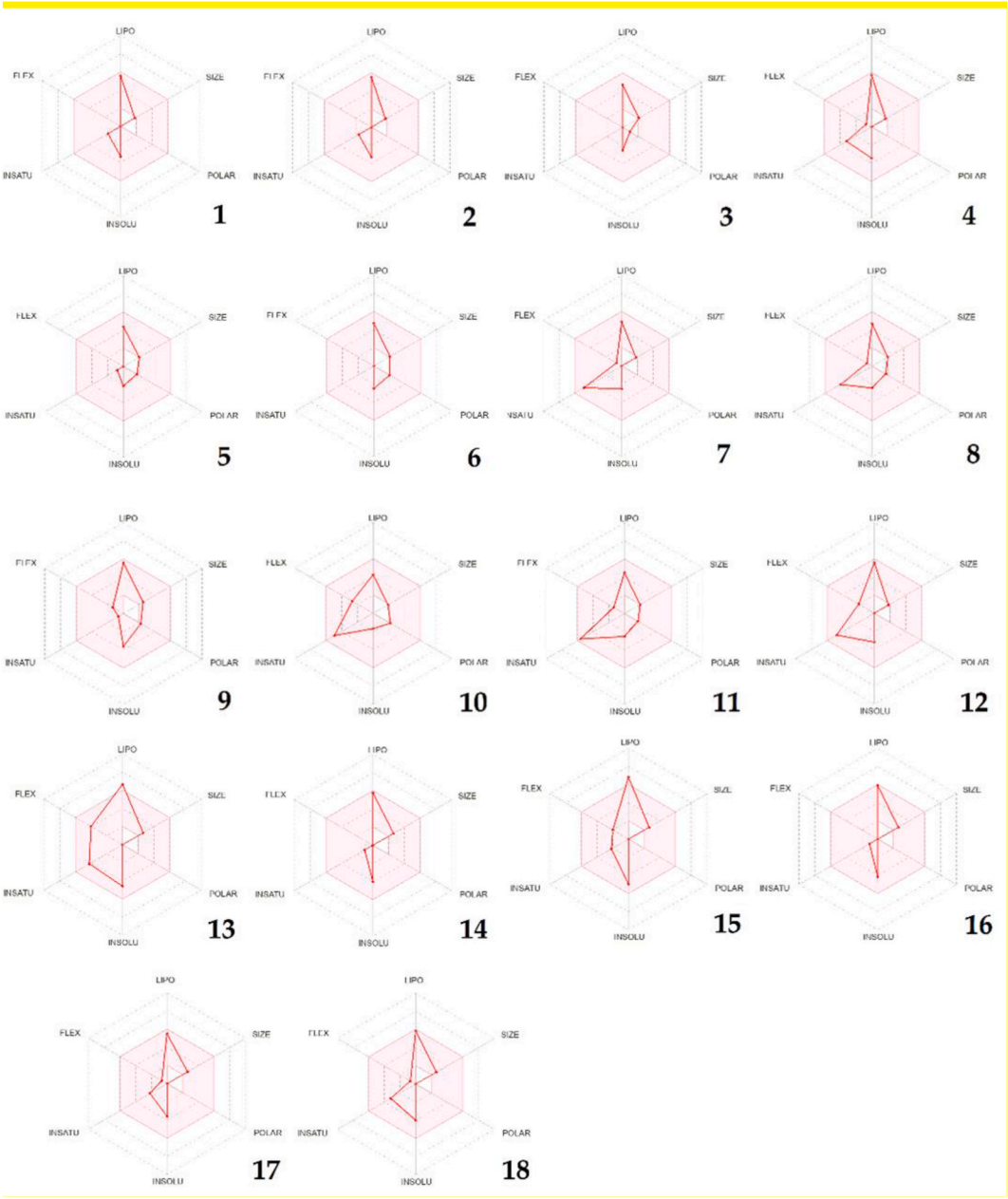

Fig. 2. LOEO compounds' bioavailability radars based on six physicochemical properties (lipophilicity, size, polarity, solubility, flexibility, and saturation). Note: **(1)** Camphene, **(2)** β−Pinene, **(3)** 1,8−cineole, **(4)** γ−Terpinene, **(5)** L−camphor, **(6)** Borneol, **(7)** 1,3,8−*p*−Menthatriene, **(8)** Carvone, **(9)** (−)−Bornyl acetate, **(10)** Allyl Tiglate, **(11)** Cuminaldehyde, **(12)** *trans*−Ocimene, **(13)** *(E)*−Farnesene, **(14)** α−Cedrene, **(15)** *(Z)*−*trans*− α−Bergamotene, **(16)** (−)−β−Funebrene, **(17)** α−Cadinene, **(18)** Germacrene D.

The pink zone on the radar graph represents the specific range within which a molecule's graphical representation must fit to be considered drug−like. This aspect is of utmost importance when assessing the molecule's potential as a therapeutic drug, as it indicates how effectively the molecule can be absorbed and distributed within the body. By utilizing bioavailability radars, we gain valuable insights into the oral bioavailability of these compounds, aiding in the identification of promising candidates for further drug development and potential therapeutic applications. In this current study, all the phytocompounds were found to fall within the appropriate range for oral bioavailability, as indicated earlier.

The BOILED−Egg model serves as a tool for an initial evaluation of a molecule's potential to be absorbed by the intestines and penetrate the blood−brain barrier (Fig. 3). It relies on two essential criteria: lipophilicity, which is gauged by WLOGP, and polarity, which is measured by TPSA [66]. The visual representation of the resulting model shows the white area indicating molecules with higher chances of absorption by the intestines, and the yellow area within the yolk representing molecules that are more likely to penetrate the blood−brain barrier [66]. In the diagram, the dots are color−coded to distinguish between molecules that act as substrates and those that do not for P−glycoprotein. Substrates are represented by blue dots, while non−substrates are represented by red dots. In this scenario, none of the tested compounds are substrates for P−glycoprotein, while all the phytocompounds have been identified as exhibiting high levels of absorption and effective crossing of the blood−brain barrier, six compounds were the exception for having a high WLOGP, (E)−Farnesene, α−Cedrene, *(Z)−trans*−α−Bergamotene, (−)−β−Funebrene, α−Cadinene, Germacrene D.

3.3. PASS prediction

Table 5 presents the results of PASS (Prediction of Activity Spectra for Substances) predictions for the major compounds found in LOEO. The table lists 18 compounds along with the tested biological activities *in silico*, including antioxidant, anti−inflammatory, and antidiabetic properties. The biological activities are represented by two parameters: Pa (probability 'to be active') and Pi (probability 'to be inactive'). Among the compounds, Camphene and β−Pinene do not show significant probabilities for any of the assessed biological activities. On the other hand, 1,8−cineole, L−camphor, Borneol, 1,3,8−p−Menthatriene, Carvone, (−)−Bornyl acetate, Allyl Tiglate, Cuminaldehyde, *trans*−Ocimene, and (E)−Farnesene exhibit varying probabilities for different activities. Notably, *trans*−Ocimene and (E)−Farnesene have higher probabilities (Pa >0.50) for being active in multiple activities, indicating their potential significance as bioactive compounds. The absence of data for some compounds, such as γ−Terpinene, α−Cedrene, (Z)−*trans*−α−Bergamotene, (−)−β−Funebrene, α−Cadinene, and Germacrene D, suggests a lack of sufficient evidence or information to assess their biological activities using PASS predictions. The information in Table 5 offers valuable insights into the potential bioactivities of the major compounds present in LOEO. However, it is essential to complement these predictions with more accurate *in silico* methods and experimental studies to confirm the actual biological activities of these compounds in the context of LOEO's therapeutic effects.

3.4. In silico toxicity prediction (using Pro−Tox II)

Table 6 provides essential insights into the potential toxicity of major compounds found in LOEO using computational models. The table presents Predicted LD_{50} values, toxicity predictions, and probabilities for various toxic endpoints. The study aimed to assess the toxicity of 18 compounds found in LOEO using computational models in the webserver Pro−Tox II [34,35]. The Predicted LD_{50} values represent the estimated lethal dose required to cause death in 50 % of a test population. Based on the LD_{50} values, compounds 1, 2, 3, 4, 9, 10, 13, 14, 15, 16, 17, and 18 are predicted to have low acute toxicity. On the other hand, compound 12 (*trans*−Ocimene) is expected

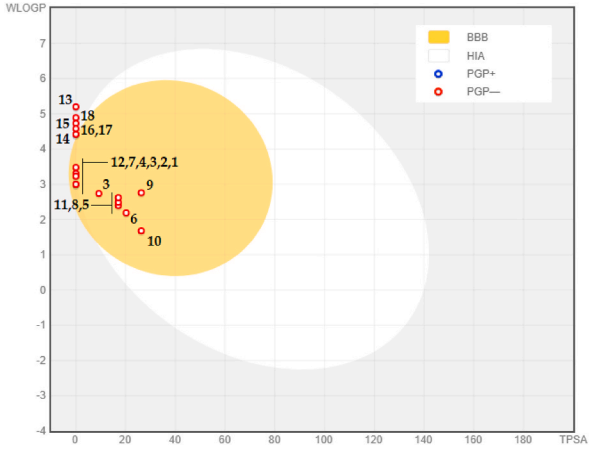

Fig. 3. BOILED−EGG model, used to assess the composition of LOEO in terms of blood−brain barrier permeability, gastrointestinal absorption, and whether the molecules act as substrates or inhibitors of P−glycoprotein. **(1)** Camphene, **(2)** β−Pinene, **(3)** 1,8−cineole, **(4)** γ−Terpinene, **(5)** L−camphor, **(6)** Borneol, **(7)** 1,3,8−*p*−Menthatriene, **(8)** Carvone, **(9)** (−)−Bornyl acetate, **(10)** Allyl Tiglate, **(11)** Cuminaldehyde, **(12)** *trans*−Ocimene, **(13)** *(E)*−Farnesene, **(14)** α−Cedrene, **(15)** *(Z)−trans*− α−Bergamotene, **(16)** (−)−β−Funebrene, **(17)** α−Cadinene, **(18)** Germacrene D.

Table 5
PASS prediction of the major compounds found in LOEO. **(1)** Camphene, **(2)** β−Pinene, **(3)** 1,8−cineole, **(4)** γ−Terpinene, **(5)** L−camphor, **(6)** Borneol, **(7)** 1,3,8−*p*−Menthatriene, **(8)** Carvone, **(9)** (−)−Bornyl acetate, **(10)** Allyl Tiglate, **(11)** Cuminaldehyde, **(12)** *trans*−Ocimene, **(13)** (E)−Farnesene, **(14)** α−Cedrene, **(15)** (Z)−*trans*− α−Bergamotene, **(16)** (−)−β−Funebrene, **(17)** α−Cadinene, **(18)** Germacrene D.

	Compounds	Biological activities					
		Antioxidant		Antiinflammatory		Antidiabetic	
		P_a	P_i	P_a	P_i	P_a	P_i
1	Camphene	–	–	0.287	0.100	0.166	0.036
2	β−Pinene	–	–	**0.611**	0.029	0.184	0.024
3	1,8−cineole	0.161	0.090	0.327	0.046	0.165	0.037
4	γ−Terpinene	–	–	0.470	0.066	–	–
5	L−camphor	0.192	0.060	0.369	0.019	0.134	0.083
6	Borneol	0.203	0.054	**0.538**	0.046	0.161	0.040
7	1,3,8−*p*−Menthatriene	0.148	0.106	0.306	0.066	0.143	0.065
8	Carvone	0.193	0.059	0.473	0.065	0.317	0.031
9	(−)−Bornyl acetate	0.334	0.018	**0.580**	0.036	0.184	0.024
10	Allyl Tiglate	0.317	0.020	0.494	0.059	–	–
11	Cuminaldehyde	0.187	0.064	0.258	0.203	0.178	0.164
12	Trans−Ocimene	**0.570**	0.005	**0.599**	0.032	0.130	0.109
13	(E)−Farnesene	**0.634**	0.004	**0.669**	0.020	0.178	0.165
14	α−Cedrene	–	–	0.358	0.118	–	–
15	(Z)− *trans*−α−Bergamotene	0.319	0.020	**0.614**	0.029	–	–
16	(−)−β−Funebrene	–	–	**0.584**	0.035	–	–
17	α−Cadinene	–	–	**0.619**	0.028	–	–
18	Germacrene D	–	–	0.457	0.070	0.127	0.101

Pa, probability 'to be active'; *Pi,* probability 'to be inactive'. Bold number: indicate a probable activity >0.50.

to have higher acute toxicity. GHS hazard classes are also provided to classify the compounds based on their LD_{50} values. The majority of compounds fall into hazard classes IV and V, indicating that most of the compounds may be harmful if swallowed. Trans−Ocimene (12) falls into hazard class III, suggesting toxicity if swallowed. The predicted toxicity endpoints offer valuable insights into the potential health effects associated with exposure to these compounds.

The endpoints examined include hepatotoxicity, mutagenicity, carcinogenicity, immunotoxicity, and cytotoxicity. Among the compounds, only numbers 16 and 18 show the highest probabilities of immunotoxicity, with probabilities of being immunotoxic compounds of 0.50, and 0.80, respectively.

In summary, this research illuminates the toxic characteristics of key compounds present in LOEO and provides vital data for assessing their potential risks. It also offers valuable input for devising strategies to minimize potential health hazards linked to the consumption of LOEO. The findings indicate that the essential oil under study might be deemed safe for oral consumption. However, it is important to note that while the results provide valuable insights into potential health effects associated with exposure to these compounds, additional *in vitro* and *in vivo* investigations are imperative to validate their actual toxicity in humans.

Table 6
Prediction of toxicity, and the toxic endpoints of the major compounds found in LOEO.

N	Predicted LD_{50} (mg/kg)	Class	Hepatotoxicity		Carcinogenicity		Immunotoxicity		Mutagenicity		Cytotoxicity	
			Predi.*	Prob.	Predi.	Prob.	Predi.	Prob.	Predi.	Prob.	Predi.	Prob.
1	5000	V	Ina.	0.79	Ina.	0.56	Ina.	0.95	Ina.	0.91	Ina.	0.76
2	4700	V	Ina.	0.80	Ina.	0.66	Ina.	0.97	Ina.	0.95	Ina.	0.71
3	2480	V	Ina.	0.86	Ina.	0.68	Ina.	0.99	Ina.	0.96	Ina.	0.75
4	2500	V	Ina.	0.83	Ina.	0.60	Ina.	0.98	Ina.	0.92	Ina.	0.82
5	775	IV	Ina.	0.72	Ina.	0.68	Ina.	0.96	Ina.	0.94	Ina.	0.61
6	500	IV	Ina.	0.77	Ina.	0.78	Ina.	0.99	Ina.	0.98	Ina.	0.88
7	1680	IV	Ina.	0.74	Ina.	0.63	Ina.	0.95	Ina.	0.89	Ina.	0.84
8	1640	IV	Ina.	0.65	Ina.	0.83	Ina.	0.99	Ina.	0.97	Ina.	0.80
9	3100	V	Ina.	0.58	Ina.	0.62	Ina.	0.94	Ina.	0.94	Ina.	0.67
10	5000	V	Ina.	0.70	Ina.	0.52	Ina.	0.99	Ina.	0.89	Ina.	0.79
11	1320	IV	Ina.	0.71	Ina.	0.52	Ina.	0.96	Ina.	0.97	Ina.	0.89
12	113	III	Ina.	0.83	Ina.	0.51	Ina.	0.99	Ina.	0.90	Ina.	0.75
13	3650	V	Ina.	0.79	Ina.	0.73	Ina.	0.99	Ina.	0.98	Ina.	0.81
14	5000	V	Ina.	0.83	Ina.	0.70	Ina.	0.98	Ina.	0.83	Ina.	0.74
15	3700	V	Ina.	0.85	Ina.	0.76	Ina.	0.94	Ina.	0.88	Ina.	0.71
16	5000	V	Ina.	0.83	Ina.	0.68	**Act.**	**0.50**	Ina.	0.86	Ina.	0.71
17	4400	V	Ina.	0.83	Ina.	0.80	Ina.	0.68	Ina.	0.60	Ina.	0.76
18	5300	V	Ina.	0.80	Ina.	0.73	**Act.**	**0.80**	Ina.	0.87	Ina.	0.83

GHS hazard classes: III: 50 mg/kg < LD_{50} < 300 mg/kg, toxic if swallowed; **IV:** 300 mg/kg < LD_{50} ≤ 2000 mg/kg, harmful if swallowed; **V:** 2000 mg/kg < LD_{50} ≤ 5000 mg/kg, may be harmful if swallowed; **VI:** LD_{50} > 5000 mg/kg, non−toxic compounds. Act: Active; Ina: Inactive.

3.5. Molecular docking analysis

Molecular docking, a powerful computational technique, is frequently employed to gain valuable insights into the molecular processes of pharmacologically active drugs [67,68]. In this particular study, we have utilized molecular docking to investigate the potential mechanism of action responsible for the anti−inflammatory properties found in the components of LOEO. By examining binding affinity values, the study aimed to determine whether the studied molecules exhibited a higher or lower affinity toward a specific target protein in comparison to a known inhibitor (native ligand). Typically, a decrease in binding energy suggests an increase in compound affinity. To present the docking scores effectively, we have employed a heat−map−type table using a three−color scheme (red−yellow−green). The color range varied from the lowest energy values, highlighted in red (usually corresponding to the docking score of the native ligand), to the highest energy values, highlighted in green. This approach facilitated the identification of chemical compounds that potentially functioned as inhibitors, as their lowest values were compared to those of the native ligand for a specific protein.

The primary aim of this method was to evaluate how 18 essential oil compounds bind to specific target proteins, which are associated with diabetes and inflammation. These target proteins are α−amylase [43], α−Glucosidase [44], lipoxygenase (LOX) [39], tyrosinase [40], human cyclooxygenase−2 (COX−2) [41], ovine cyclooxygenase 1 (COX−1) [42], identified by PDB IDs: 1SMD, 5NN5, 1N8Q, 5I3B, 5IKV, 5WBE, respectively.

α-Glucosidase functions as a crucial digestive enzyme primarily responsible for expediting the breakdown of polysaccharides, particularly starch, into glucose by cleaving (14) bonds. This process facilitates glucose absorption, ultimately leading to an increase in blood glucose levels [69,70]. By regulating the degradation of starch and other dietary carbohydrates, this enzyme plays a role in preventing hyperglycemia and maintaining optimal blood sugar levels [69,70]. Through enzymatic hydrolysis, alpha-glucosidase significantly enhances the absorption of simple sugars, such as glucose, derived from starch and dietary carbohydrates within the intestines, resulting in elevated blood glucose levels [71]. Among all the ligands evaluated, only (E)-Farnesene exhibited a notable affinity for the enzyme's active site (PDB ID: 5NN5), showing the most prominent affinity of −7.4 kcal/mol, equivalent to that of the native ligand (acarbose; −7.4 kcal/mol). Inhibiting the proper function of this enzyme has the potential to assist in alleviating postprandial hyperglycemia.

α-Amylase, functions as a catalyst in breaking down α-linked polysaccharides into α-anomeric products through hydrolysis [72]. This enzyme plays a vital role in carbohydrate digestion. It is present and active both in pancreatic juice and saliva [73]. The active site of α-amylase (PDB ID: 1SMD) comprises three catalytic residues: Asp197, Glu233, and Asp300. Additionally, several other residues contribute significantly to the enzyme's activity, including Arg337, Arg195, Asn298, Phe265, Phe295, His201, Ala307, Gly306, Trp203, Trp284, Trp59, Tyr62, Trp58, His299, and His101 [73–75]. Among various tested ligands, only three exhibited affinities comparable to the native ligand (acarbose; −7.8 kcal/mol) for the active site. Germacrene D (18) demonstrated the highest affinity among these ligands (−7.9 kcal/mol).

Tyrosinase plays a pivotal role as the chief regulatory enzyme within the melanin biosynthesis pathway, particularly in the initial two stages: (i) the conversion of tyrosine to 3,4-dihydroxyphenylalanine (DOPA), and (ii) the oxidation of DOPA to dopaquinone [20]. In the docking investigations and calculations of binding free energy, α-Cadinene demonstrated the highest interaction energy with tyrosinase (PDB ID: 5I3B), at −6 kcal/mol. Notably, among the 18 ligands assessed, 8 ligands (7, 8, 11, 14, 15, 16, 17, and 18) displayed a strong affinity for the targeted protein, in comparison with the native inhibitor of tyrosinase, hydroquinone (with a free binding energy of −5.5 kcal/mol).

Overproduction of mediators of the arachidonic acid (AA) cascade, particularly those of the cyclooxygenase (COX) and lipoxygenase (LOX) pathways, causes major inflammatory diseases in humans [71]. Lipoxygenase (LOX) is a kind of rate-limiting enzyme in the process of arachidonic acid metabolism into leukotriene (LT) which mediates the occurrence of inflammation. The inhibition of LOX can reduce LT, thereby producing an anti-inflammatory effect [71]. Four ligands were found to have a strong inhibitory potential, namely, (−)−Bornyl acetate (9), α−Cedrene (14), (−)−β−Funebrene (16), and α−Cadinene (17), with −6.1, −6.5, −6.3, and −6.4 kcal/mol, respectively, in comparison with protocatechuic acid with −5.5 kcal/mol.

The two cyclooxygenase enzymes exhibit a significant level of similarity, sharing 61 % sequence identity overall and 78 % identity when considering only the active site residues [76]. COX enzymes are homodimers, composed of two closely connected monomers, and each monomer comprises three domains: the epidermal growth factor domain, the membrane binding domain, and the catalytic domain housing the cyclooxygenase active site [77]. Previous crystallographic studies have revealed that COX enzymes possess an extended hydrophobic channel connecting the membrane binding domain to the active site. The entrance of this channel is broad, but it gradually narrows down, forming a constriction comprising three critical residues − Arg120, Tyr355, and Glu524 − which create a hydrogen−bonding network [42,77]. Despite having similar active sites, COX−2 has an additional side pocket surrounded by Val523 (unlike Ile523 in COX−1) located above Arg120 and Tyr355. This leads to an increased available space within the active site. Additionally, COX−2 reserves Arg513 (replacing His513 in COX−1) [78]. In the docking simulation study of the identified compounds in Lavender Essential Oil (LOEO) with the active sites of COX−2 and COX−1 enzymes, several metabolites showed promising inhibitory activity. Specifically, three metabolites, α−Cedrene (14), (−)−β−Funebrene (16), and Germacrene D (18), demonstrated potent inhibitory potential against COX−2, with free binding energy values of −7.3, −7.2, and −7.0 kcal/mol, respectively. These values were compared with the native ligand, Flufenamic acid, which exhibited a binding energy of −6.9 kcal/mol. Moreover, in the docking simulation of the identified compounds with the active site of COX−1 enzyme, two compounds, α−Cedrene (14), and α−Cadinene (17), exhibited strong potential to inhibit the enzyme COX−1, with binding energy values of −7.6 and −7.5 kcal/mol, respectively (Table 7). These results were compared with the native inhibitor, Mofezolac, which showed a docking score of −7.7 kcal/mol. The findings suggest that these specific metabolites in LOEO have the potential to act as effective inhibitors for the respective

target enzymes, making them promising candidates for further exploration in the development of new therapeutic agents targeting inflammation and related processes.

3.6. Experimental validation

3.6.1. α−Amylase and α−Glucosidase inhibitory activities

The management of metabolic disorders involves a multifaceted medical approach, tailored to the specific type of disorder. For treating type 2 diabetes, one common strategy is to inhibit the enzymes responsible for carbohydrate hydrolysis, such as α−amylase and α−glucosidase. In the human digestive system, α−amylase breaks down complex carbohydrates into shorter oligosaccharides, while α−glucosidase further breaks down disaccharides into simpler monosaccharides. By blocking the action of these enzymes, the breakdown of polysaccharides is reduced, leading to slower glucose absorption in the intestine and a more gradual increase in blood glucose levels after meals. This approach is particularly useful for managing postprandial blood glucose levels in individuals with type 2 diabetes or glucose intolerance.

To explore this concept, researchers evaluated the impact of LOEO on α−amylase and α−glucosidase *in vitro*. The results demonstrated that this essential oil exhibited significant inhibitory activity against both α−amylase and α−glucosidase, with IC_{50} values of 3.14 ± 0.05 mg/mL and 2.07 ± 0.03 mg/mL, respectively. However, the inhibitory activities were slightly lower than those observed for the positive control, Acarbose, which had IC_{50} values of 2.92 ± 0.06 mg/mL and 1.83 ± 0.02 mg/mL, respectively (Table 8). Despite being less potent than the positive control, the results suggest that LOEO has noteworthy inhibitory effects on these two enzymes, making it a potential source of natural antidiabetic agents due to its ability to inhibit digestive enzymes. Notably, 1,8−cineole, a major compound in LOEO, has previously been studied for its remarkable anti−diabetic effect [79]. Carvone, another compound in the essential oil, has also shown significant anti−diabetic activity according to previous studies [80,81]. Other molecules present in smaller quantities could also contribute to the essential oil's anti−diabetic activity through synergistic effects [82]. Taken together, these findings indicate that LOEO holds promise as a natural compound for the development of therapeutic drugs targeting type 2 diabetes.

3.6.2. Anti-inflammatory activities of LOEO

Lipoxygenase (LOX) and tyrosinase play a pivotal role in the progression of diseases, particularly within the context of inflammatory processes. Inhibiting their activity stands as a pivotal strategy in the prevention of these diseases. Remarkably, LOEO has been documented for the first time to exhibit notable *in vitro* anti-inflammatory effects against both LOX and tyrosinase. The ensuing outcomes are comprehensively outlined in a tabulated format, revealing the substantial anti-inflammatory efficacy of LOEO (Fig. 4).

Table 7
Heat map of the docking scores (binding free energy values are expressed in kcal/mol) of LOEO oils components: 5IKV, human cyclooxygenase−2 (COX−2); 5WBE, ovine cyclooxygenase 1 (COX−1); 1N8Q: Lipoxygenase (LOX); 5I3B: Tyrosinase; 5NN5: α-glucosidase; 1SMD: α-amylase.

N°	Compounds	5IKV	5WBE	1N8Q	5I3B	5NN5	1SMD
		Free Binding Energy ΔG (kcal/mol) [1]					
–	Native Ligand	−6.9	−7.7	−6	−5.5	−7.4	−7.8
1	Camphene	−5.3	−5.1	−4.7	−4.6	−5.7	−5.5
2	β−Pinene	−5.2	−5.3	−4.8	−4.6	−5.4	−5.4
3	1,8−cineole	−5.5	−5.8	−5.5	−4.8	−5.3	−5.4
4	γ−Terpinene	−5.4	−5.7	−5.1	−4.8	−5.4	−6
5	L−camphor	−5.6	−5.6	−5.3	−4.9	−5.2	−5.5
6	Borneol	−5.3	−5.4	−5.3	−5	−5.2	−5.5
7	1,3,8−*p*−Menthatriene	−5.7	−5.0	−5.9	−5.7	−5.4	−6
8	Carvone	−6.0	−6.2	−5.4	−5.5	−5.8	−5.9
9	(−)−Bornyl acetate	−6.1	−5.9	−6.1	−5.3	−5.4	−6
10	Allyl Tiglate	−4.9	−5.0	−5.4	−4.9	−4.9	−4.7
11	Cuminaldehyde	−5.9	−6.1	−5.6	−5.9	−5.4	−6.1
12	*trans*−Ocimene	−5.0	−5.2	−5.2	−4.3	−5.2	−5.3
13	(E)−Farnesene	−5.8	−5.7	−5.6	−5.3	−7.4	−5.6
14	α−Cedrene	−7.3	−7.6	−6.5	−5.6	−7	−7.1
15	(Z)−*trans*−α−Bergamotene	−6.5	−6.2	−5.9	−5.6	−6	−6.6
16	(−)−β−Funebrene	−7.2	−6.7	−6.3	−5.5	−6.1	−7.7
17	α−Cadinene	−6.7	−7.5	−6.4	−6	−6.3	−7.5
18	Germacrene D	−7.0	−6.7	−5.9	−5.8	−7.1	−7.9

[1] For each column, the color scale ranges from red (referring to the native ligand ΔG), through yellow (mid−point), to green (native ligand ΔG + 5 kcal/mol).

Table 8
The antidiabetic activity of LOEO (IC_{50} in mg/mL). The results are presented as means ± SD (standard deviations) for triplicate assays.

Enzymes	LOEO	Acarbose
	IC_{50} (mg/ml)	
α−amylase	3.14 ± 0.05	2.92 ± 0.06
α−glucosidase	2.07 ± 0.03	1.83 ± 0.02

Specifically, LOEO demonstrated remarkable inhibition against the LOX enzyme, displaying an IC_{50} value of 11.58 ± 0.07 μg/mL. Comparative analysis of our findings with those from other members of the Lamiaceae Family, to which *L. officinalis* belongs, underscores the superior performance of LOEO. Notably, when considering extracts from *Clerodendrum disparifolium* Blume leaves, the ethanolic and *n*-Hexanic extracts exhibited IC_{50} values of 24.39 μg/mL and 30.56 μg/mL, respectively.

Likewise *Clerodendrum laevifolium* Blume Leaves the ethanolic and *n*-Hexanic extracts have been dipected IC_{50} value of 14.12 μg/mL and 30.70 μg/mL respectively [83]. Futhermore for anti-tyrosinase activity the LOEO shown significant IC_{5O} value of 42.74 μg/mL. If we want to compare it with the species of its family specifically with-it genus as like as *L. stoechas* subsp. *pedunculata*, *L. latifolia* and *L. allardii* 'Rly' which shown the IC_{50} value of 0.13 mg/mL, 0.15 mg/mL, 0.11 mg/mL respectively [84]. This result proves the higher anti-inflammatory potential of LOEO that which line promising therapeutic arsenal.

The biological properties of a LOEO components are generally related to their chemical structure, especially the presence and arrangement of functional groups such as hydroxyl groups, esters, and alkenes.

Indeed, hydroxyl groups (-OH) are known to influence the solubility, membrane permeability, and interactions with biological targets of organic compounds. The presence of hydroxyl groups enhances the compound's solubility in aqueous environments by facilitating hydrogen bonding with water molecules [85]. This increased solubility can lead to improved bioavailability and distribution within the body, enhancing the compound's biological potential. On the other hands, –OH can participate in hydrogen bonding interactions with polar residues on the surface of biological targets such as enzymes or receptors [86]. These interactions can influence the binding affinity and specificity of the compound to its target, ultimately modulating its biological activity. Additionally, hydroxyl

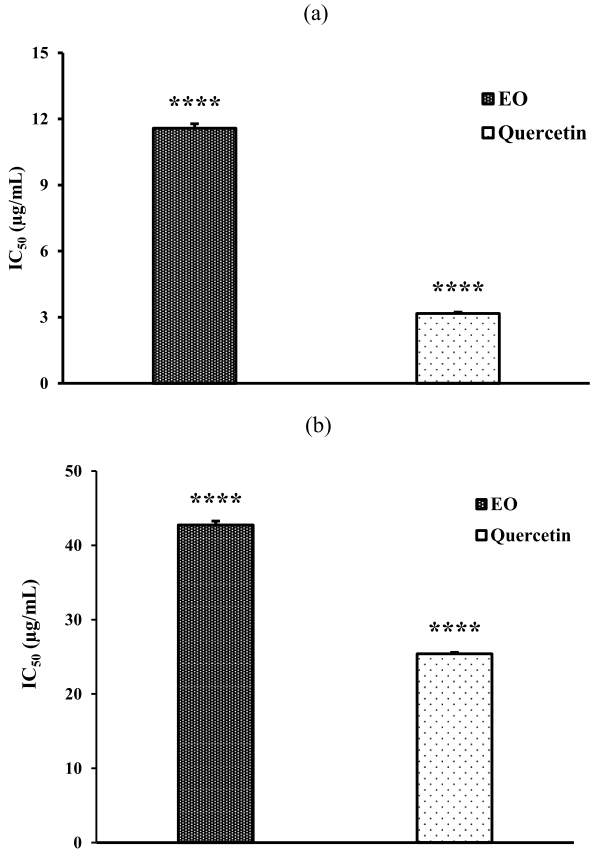

Fig. 4. Anti-inflammatory and dermatoprotective activities of LOEO against (a) LOX-5 and (b) tyrosinase. Quercetin was used as a control. Data are represented as means ± SD (n = 3). ***** p-value <0.01.

groups may affect membrane permeability by altering the polarity and lipophilicity of the compound, thereby influencing its ability to traverse biological membranes [87].

Furthermore, Esters are another important class of functional groups that can impact the health benefits and biological effects of a compound. The presence of ester groups can affect the compound's solubility profile, with smaller esters being more soluble in aqueous environments due to their ability to form hydrogen bonds with water molecules [86]. However, larger esters may exhibit decreased water solubility and increased lipophilicity, affecting their distribution and metabolism *in vivo*. In addition, ester groups can enhance membrane permeability by facilitating the diffusion of the compound across lipid bilayers [88]. The lipophilic nature of esters allows them to partition into the hydrophobic interior of cell membranes, promoting their passage into cells. This increased membrane permeability can influence the compound's ability to reach intracellular targets and exert its pharmacological effects.

Alkenes, characterized by carbon-carbon double bonds, also play a crucial role in determining the biological properties of given compounds. While alkenes are generally nonpolar and hydrophobic, their presence can influence the compound's solubility in both aqueous and lipid environments. Alkenes may exhibit low solubility in water but are soluble in nonpolar solvents due to their hydrophobic nature. Additionally, alkenes can enhance membrane permeability via simplifying passive diffusion through lipid bilayers [88]. The nonpolar nature of alkenes allows them to partition into the hydrophobic core of cell membranes, permitting their rapid transport across membranes. This events altered compound's bioavailability, influencing then its bioactivity [86].

4. Conclusions

In this study, we elucidated the chemical composition of LOEO and its diverse biological activities, including antidiabetic, anti-inflammatory, and dermatoprotective effects, employing a combination of computational and *in vitro* experimental methodologies. GC-MS analysis revealed a rich array of biologically active compounds within LOEO, predominantly comprising monoterpenes hydrocarbons and oxygenated derivatives, with camphor and 1,8-cineol identified as the primary constituents. Computational investigations demonstrated the efficacy of these EO-derived compounds in targeting established anti-diabetic and anti-inflammatory proteins. These findings were corroborated by *in vitro* experiments, confirming the potent anti-diabetic, anti-inflammatory, and dermatoprotective properties of LOEO. These results suggest the potential utility of LOEO in the development of novel biopharmaceutical products targeting diabetes and inflammation-related disorders. Moreover, the intricate interaction between EO compounds and protein targets offers valuable insights for future research, facilitating the advancement of innovative therapeutic strategies in this domain.

CRediT authorship contribution statement

Hamza Assaggaf: Writing – review & editing, Project administration, Conceptualization. **Naoufal El Hachlafi:** Writing – original draft, Project administration. **Amine Elbouzidi:** Writing – review & editing, Formal analysis. **Mohamed Taibi:** Writing – original draft, Project administration, Methodology. **Sulaiman Mohammed Alnasser:** Writing – original draft, Validation, Methodology. **Hajar Bendaif:** Writing – original draft, Software. **Youssra Aalilou:** Writing – original draft, Software, Resources. **Ahmed Qasem:** Writing – original draft, Supervision, Formal analysis. **Ammar Attar:** Writing – original draft, Formal analysis, Data curation. **Abdelhakim Bouyahya:** Writing – original draft, Software, Methodology, Investigation. **Chrismawan Ardianto:** Writing – review & editing, Validation, Software, Investigation. **Long Chiau Ming:** Writing – original draft, Software, Resources, Methodology, Conceptualization. **Khang Wen Goh:** Writing – review & editing, Resources, Investigation. **Kawtar Fikri-Benbrahim:** Writing – original draft, Project administration, Conceptualization. **Hanae Naceiri Mrabti:** Writing – original draft, Resources, Methodology.

Declaration of competing interest

The authors declare that they have no known competing financial interests or personal relationships that could have appeared to influence the work reported in this paper.

Acknowledgments

The authors extend their appreciation to the Deanship for Research & Innovation, Ministry of Education in Saudi Arabia for funding this research work through the project number: IFP22UQU4310026DSR012.

References

[1] S. Tsalamandris, A.S. Antonopoulos, E. Oikonomou, G.-A. Papamikroulis, G. Vogiatzi, S. Papaioannou, S. Deftereos, D. Tousoulis, The role of inflammation in diabetes: current concepts and future perspectives, Eur. Cardiol. 14 (2019) 50.
[2] E. Lontchi-Yimagou, E. Sobngwi, T.E. Matsha, A.P. Kengne, Diabetes mellitus and inflammation, Curr. Diabetes Rep. 13 (2013) 435–444.
[3] B.S. Nikolajczyk, M. Jagannathan-Bogdan, H. Shin, R. Gyurko, State of the union between metabolism and the immune system in type 2 diabetes, Gene Immun. 12 (2011) 239–250.
[4] S.E. Shoelson, J. Lee, A.B. Goldfine, Inflammation and insulin resistance, J. Clin. Investig. 116 (2006) 1793–1801.
[5] Y.-Y. Yang, L.-X. Shi, J.-H. Li, L.-Y. Yao, D.-X. Xiang, Piperazine ferulate ameliorates the development of diabetic nephropathy by regulating endothelial nitric oxide synthase, Mol. Med. Rep. 19 (2019) 2245–2253.
[6] R. Chen, S. Xu, Y. Ding, L. Li, C. Huang, M. Bao, S. Li, Q. Wang, Dissecting causal associations of type 2 diabetes with 111 types of ocular conditions: a Mendelian randomization study, Front. Endocrinol. 14 (2023) 1307468.

[7] Z. Zuberi, E. Sauli, L. Cun, J. Deng, W.-J. Li, X.-L. He, W. Li, Insulin-delivery methods for children and adolescents with type 1 diabetes, Therapeutic Advances in Endocrinology and Metabolism 11 (2020) 2042018820906016.

[8] J. Chen, X. Li, H. Liu, D. Zhong, K. Yin, Y. Li, L. Zhu, C. Xu, M. Li, C. Wang, Bone marrow stromal cell-derived exosomal circular RNA improves diabetic foot ulcer wound healing by activating the nuclear factor erythroid 2-related factor 2 pathway and inhibiting ferroptosis, Diabet. Med. 40 (2023) e15031.

[9] S. Singh, A.S. Chishti, S. Singh, U.H. Bhat, M. Uddin, Bioactive compounds and pharmacological values of Lavandula angustifolia (Syn. L. officinalis Chaix), in: Bioactives and Pharmacology of Medicinal Plants, Apple Academic Press, 2022, pp. 215–224.

[10] B. Rahmati, M. Khalili, M. Roghani, P. Ahghari, Anti-epileptogenic and antioxidant effect of Lavandula officinalis aerial part extract against pentylenetetrazol-induced kindling in male mice, J. Ethnopharmacol. 148 (2013) 152–157.

[11] G. Kaka, K. Yaghoobi, S. Davoodi, S.R. Hosseini, S.H. Sadraie, K. Mansouri, Assessment of the neuroprotective effects of lavandula angustifolia extract on the contusive model of spinal cord injury in wistar rats, Front. Neurosci. 10 (2016) 25.

[12] R. Alnamer, K. Alaoui, E.H. Bouidida, A. Benjouad, Y. Cherrah, Sedative and hypnotic activities of the methanolic and aqueous extracts of Lavandula officinalis from Morocco, Advances in Pharmacological and Pharmaceutical Sciences 2012 (2012).

[13] R. Alnamer, K. Alaoui, E. Houcine Bouidida, A. Benjouad, Y. Cherrah, Toxicity and psychotropic activity of essential oils of Rosmarinus officinalis and Lavandula officinalis from Morocco, Journal of Biologically Active Products from Nature 1 (2011) 262–272.

[14] S. Garzoli, V. Laghezza Masci, S. Franceschi, A. Tiezzi, P. Giacomello, E. Ovidi, Headspace/GC–MS analysis and investigation of antibacterial, antioxidant and cytotoxic activity of essential oils and hydrolates from Rosmarinus officinalis L. and Lavandula angustifolia Miller, Foods 10 (2021) 1768.

[15] N. El Hachlafi, H.N. Mrabti, S.H. Al-Mijalli, M. Jeddi, E.M. Abdallah, N. Benkhaira, H. Hadni, H. Assaggaf, A. Qasem, K.W. Goh, Antioxidant, volatile compounds; antimicrobial, anti-inflammatory, and dermatoprotective properties of Cedrus atlantica (Endl.) Manetti Ex Carriere essential oil: in vitro and in silico investigations, Molecules 28 (2023) 5913.

[16] H. Rostami, M. Kazemi, S. Shafiei, Antibacterial activity of Lavandula officinalis and Melissa officinalis against some human pathogenic bacteria, Asian J. Biochem. 7 (2012) 133–142.

[17] H. Demir, S. Kalaycı, Chemical composition and antimicrobial activity of essential oils of Ocimum basilicum var. album (L.) Benth, Lavandula angustifolia subsp. Angustifolia, Melissa officinalis belonging to Lamiaceae family, J. Food Sci. Educ. 7 (2017) 461–471.

[18] K. Diass, F. Brahmi, O. Mokhtari, S. Abdellaoui, B. Hammouti, Biological and pharmaceutical properties of essential oils of Rosmarinus officinalis L. and Lavandula officinalis L, Mater. Today: Proc. 45 (2021) 7768–7773.

[19] S. Chaibi, K. Remla, K. Boussedjra, H.S. Nacef, Isolement, identification des champignons endophytes et extraction de l'huile essentielle de la plante médicinale Lavandula officinalis et leur activité antimicrobienne, 2021.

[20] D.H. Abou Baker, R. Amarowicz, A. Kandeil, M.A. Ali, E.A. Ibrahim, Antiviral activity of Lavandula angustifolia L. and Salvia officinalis L. essential oils against avian influenza H5N1 virus, Journal of Agriculture and Food Research 4 (2021) 100135.

[21] Y. Husseini, H. Sahraei, G.H. Meftahi, M. Dargahian, A. Mohammadi, B. Hatef, H. Zardooz, M. Ranjbaran, S.B. Hosseini, H. Alibeig, Analgesic and anti-inflammatory activities of hydro-alcoholic extract of Lavandula officinalis in mice: possible involvement of the cyclooxygenase type 1 and 2 enzymes, Revista Brasileira de Farmacognosia 26 (2016) 102–108.

[22] M. Slighoua, M. Chebaibi, I. Mahdi, F.E. Amrati, R. Conte, M.A.W. Cordero, A. Alotaibi, H. Saghrouchni, A. Agour, T. Zair, The LC-MS/MS identification and analgesic and wound healing activities of Lavandula officinalis Chaix: in vivo and in silico approaches, Plants 11 (2022) 3222.

[23] M.A. Fahmy, A.A. Farghaly, E.E. Hassan, E.M. Hassan, Z.M. Hassan, K. Mahmoud, E.A. Omara, Evaluation of the anti-cancer/anti-mutagenic efficiency of Lavandula officinalis essential oil, Asian Pac. J. Cancer Prev. APJCP 23 (2022) 1215.

[24] A. Abdanipour, R. Nejatbakhsh, I. Jafari Anarkooli, M. Ghorbanlo, A. Nikfar, A. Noriyan, Prolifration and anti-apoptotic effect of hydroethanolic extract of Lavandula officinalis on rat neural stem cells, Journal of Advances in Medical and Biomedical Research 24 (2016) 43–52.

[25] M. Azarmi, H. Saei, S. Zehtab Salmasi, G. Dehghan, Investigating the treatable effect of Lavandula officinalis L. Ethanolic extract in alloxan-induced male diabetic rats, Pharmacol. Line 1 (2016) 53–63.

[26] M.R. González-Tejero, M. Casares-Porcel, C.P. Sánchez-Rojas, J.M. Ramiro-Gutiérrez, J. Molero-Mesa, A. Pieroni, M.E. Giusti, E. Censorii, C. De Pasquale, A. Della, Medicinal plants in the Mediterranean area: synthesis of the results of the project Rubia, J. Ethnopharmacol. 116 (2008) 341–357.

[27] N. El Hachlafi, N. Benkhaira, S.H. Al-Mijalli, H.N. Mrabti, R. Abdnim, E.M. Abdallah, M. Jeddi, M. Bnouham, L.-H. Lee, C. Ardianto, Phytochemical analysis and evaluation of antimicrobial, antioxidant, and antidiabetic activities of essential oils from Moroccan medicinal plants: Mentha suaveolens, Lavandula stoechas, and Ammi visnaga, Biomed. Pharmacother. 164 (2023) 114937.

[28] N. Benkhaira, N. Zouine, M. Fadil, S.I. Koraichi, N.E. Hachlafi, M. Jeddi, M. Lachkar, K. Fikri-Benbrahim, Application of mixture design for the optimum antibacterial action of chemically-analyzed essential oils and investigation of the antiadhesion ability of their optimal mixtures on 3D printing material, Bioprinting (2023) e00299, https://doi.org/10.1016/j.bprint.2023.e00299.

[29] A. Elbouzidi, M. Taibi, H. Ouassou, S. Ouahhoud, D. Ou-Yahia, E.H. Loukili, M. Aherkou, F. Mansouri, N. Bencheikh, S. Laaraj, R. Bellaouchi, E. Saalaoui, K. Elfazazi, A. Berrichi, M. Abid, M. Addi, Exploring the multi-faceted potential of carob (Ceratonia siliqua var. Rahma) leaves from Morocco: a comprehensive analysis of polyphenols profile, antimicrobial activity, cytotoxicity against breast cancer cell lines, and genotoxicity, Pharmaceuticals 16 (2023) 840, https://doi.org/10.3390/ph16060840.

[30] S.H. Al-Mijalli, H.N. Mrabti, N. El Hachlafi, T. El Kamili, A. Elbouzidi, E.M. Abdallah, R. Flouchi, H. Assaggaf, A. Qasem, G. Zengin, Integrated analysis of antimicrobial, antioxidant, and phytochemical properties of Cinnamomum verum: a comprehensive in vitro and in silico study, Biochem. Systemat. Ecol. 110 (2023) 104700.

[31] A. Daina, O. Michielin, V. Zoete, SwissADME: a free web tool to evaluate pharmacokinetics, drug-likeness and medicinal chemistry friendliness of small molecules, Sci. Rep. 7 (2017) 1–13.

[32] D.E. V Pires, T.L. Blundell, D.B. Ascher, pkCSM: predicting small-molecule pharmacokinetic and toxicity properties using graph-based signatures, J. Med. Chem. 58 (2015) 4066–4072, https://doi.org/10.1021/acs.jmedchem.5b00104.

[33] S. Ouahabi, E.H. Loukili, A. Elbouzidi, M. Taibi, M. Bouslamti, H.-A. Nafidi, A.M. Salamatullah, N. Saidi, R. Bellaouchi, M. Addi, Pharmacological properties of chemically characterized extracts from mastic tree: in vitro and in silico assays, Life 13 (2023) 1393.

[34] P. Banerjee, A.O. Eckert, A.K. Schrey, R. Preissner, ProTox-II: a webserver for the prediction of toxicity of chemicals, Nucleic Acids Res. 46 (2018) W257–W263, https://doi.org/10.1093/nar/gky318.

[35] H.N. Mrabti, N. El Hachlafi, S.H. Al-Mijalli, M. Jeddi, A. Elbouzidi, E.M. Abdallah, F.O. Chahdi, Phytochemical profile, assessment of antimicrobial and antioxidant properties of essential oils of Artemisia herba-alba Asso., and Artemisia dracunculus L.: Experimental and computational approaches, J. Mol. Struct. 1294 (2023) 136479.

[36] M. Taibi, A. Elbouzidi, D. Ou-Yahia, M. Dalli, R. Bellaouchi, A. Tikent, M. Roubi, N. Gseyra, A. Asehraou, C. Hano, M. Addi, B. El Guerrouj, K. Chaabane, Assessment of the antioxidant and antimicrobial potential of Ptychotis verticillata Duby essential oil from Eastern Morocco: an in vitro and in silico analysis, Antibiotics 12 (2023), https://doi.org/10.3390/antibiotics12040655.

[37] A. Elbouzidi, M. Taibi, S. Laaraj, E.H. Loukili, M. Haddou, N. El Hachlafi, M. Addi, Chemical profiling of volatile compounds of the essential oil of grey-leaved rockrose (Cistus albidus L.) and its antioxidant, anti-inflammatory, antibacterial, antifungal, and anticancer activity in vitro and in silico, Front. Chem. 12 (2024) 1334028.

[38] C. Jianu, I. Goleț, D. Stoin, I. Cocan, G. Bujancă, C. Mișcă, M. Mioc, A. Mioc, C. Șoica, A.T. Lukinich-Gruia, L.-C. Rusu, D. Muntean, D.I. Horhat, Chemical profile of Ruta graveolens, evaluation of the antioxidant and antibacterial potential of its essential oil, and molecular docking simulations, Appl. Sci. 11 (2021), https://doi.org/10.3390/app112411753.

[39] A. Elbouzidi, H. Ouassou, M. Aherkou, L. Kharchoufa, N. Meskali, A. Baraich, H. Mechchate, M. Bouhrim, A. Idir, C. Hano, LC–MS/MS phytochemical profiling, antioxidant activity, and cytotoxicity of the ethanolic extract of Atriplex halimus L. Against breast cancer cell lines: computational studies and experimental validation, Pharmaceuticals 15 (2022) 1156, https://doi.org/10.3390/ph15091156.

[40] V. di Giacomo, L. Recinella, A. Chiavaroli, G. Orlando, A. Cataldi, M. Rapino, V. Di Valerio, M. Politi, M.D. Antolini, A. Acquaviva, F. Bacchin, M. Di Mascio, S. Leone, L. Brunetti, L. Menghini, S. Carradori, G. Zengin, G. Ak, C. Ferrante, Metabolomic profile and antioxidant/anti-inflammatory effects of industrial hemp water extract in fibroblasts, keratinocytes and isolated mouse skin specimens, Antioxidants 10 (2021), https://doi.org/10.3390/antiox10010044.
[41] B.J. Orlando, M.G. Malkowski, Substrate-selective inhibition of cyclooxygeanse-2 by fenamic acid derivatives is dependent on peroxide tone, J. Biol. Chem. 291 (2016) 15069–15081.
[42] G. Cingolani, A. Panella, M.G. Perrone, P. Vitale, G. Di Mauro, C.G. Fortuna, R.S. Armen, S. Ferorelli, W.L. Smith, A. Scilimati, Structural basis for selective inhibition of Cyclooxygenase-1 (COX-1) by diarylisoxazoles mofezolac and 3-(5-chlorofuran-2-yl)-5-methyl-4-phenylisoxazole (P6), Eur. J. Med. Chem. 138 (2017) 661–668.
[43] G.J. Fadimu, A. Farahnaky, H. Gill, O.A. Olalere, C.-Y. Gan, T. Truong, In-silico analysis and antidiabetic effect of α-amylase and α-glucosidase inhibitory peptides from lupin protein hydrolysate: enzyme-peptide interaction study using molecular docking approach, Foods 11 (2022) 3375.
[44] N.G.E.R. Etsassala, J.A. Badmus, J.L. Marnewick, S. Egieyeh, E.I. Iwuoha, F. Nchu, A.A. Hussein, Alpha-glucosidase and alpha-amylase inhibitory activities, molecular docking, and antioxidant capacities of Plectranthus ecklonii constituents, Antioxidants 11 (2022) 378.
[45] M. Rădulescu, C. Jianu, A.T. Lukinich-Gruia, M. Mioc, A. Mioc, C. Şoica, L.G. Stana, Chemical composition, in vitro and in silico antioxidant potential of Melissa officinalis subsp. officinalis essential oil, Antioxidants 10 (2021) 1081.
[46] S.S. Basak, F. Candan, Effect of Laurus nobilis L. essential oil and its main components on α-glucosidase and reactive oxygen species scavenging activity, Iran. J. Pharm. Res. (IJPR): IJPR 12 (2013) 367.
[47] A. Bouyahya, A. Et-Touys, J. Abrini, A. Talbaoui, H. Fellah, Y. Bakri, N. Dakka, Lavandula stoechas essential oil from Morocco as novel source of antileishmanial, antibacterial and antioxidant activities, Biocatal. Agric. Biotechnol. 12 (2017) 179–184.
[48] Y. El Ouadi, H. Bendaif, H. Assaggaf, E.M. Abdallah, M. Mekkaoui, H.N. Mrabti, M. Manssouri, T. Benali, A. Bouyahya, A. Bouyanzer, Efficacy of Pelargonium graveolens essential oils against some postharvest fungal diseases of apple, Advancements in Life Sciences 9 (2022) 195–201.
[49] Y. El Ouadi, M. Manssouri, A. Bouyanzer, L. Majidi, H. Bendaif, H. Elmsellem, M.A. Shariati, A. Melhaoui, B. Hammouti, Essential oil composition and antifungal activity of Melissa officinalis originating from north-Est Morocco, against postharvest phytopathogenic fungi in apples, Microb. Pathog. 107 (2017) 321–326.
[50] M. Taibi, A. Elbouzidi, S. Ouahhoud, E.H. Loukili, D. Ou-Yahya, S. Ouahabi, A.S. Alqahtani, O.M. Noman, M. Addi, R. Bellaouchi, A. Asehraou, E. Saalaoui, B. E. Guerrouj, K. Chaabane, Evaluation of antioxidant activity, cytotoxicity, and genotoxicity of Ptychotis verticillata essential oil: towards novel breast cancer therapeutics, Life 13 (2023), https://doi.org/10.3390/life13071586.
[51] M. Haddou, M. Taibi, A. Elbouzidi, E.H. Loukili, M.I. Yahyaoui, D. Ou-Yahia, L. Mehane, M. Addi, A. Asehraou, K. Chaabane, R. Bellaouchi, B. El Guerrouj, Investigating the impact of irrigation water quality on secondary metabolites and chemical profile of Mentha piperita essential oil: analytical profiling, characterization, and potential pharmacological applications, Int. J. Plant Biol. 14 (2023) 638–657, https://doi.org/10.3390/ijpb14030049.
[52] M. Hayani, N. Bencheikh, A. Ailli, M. Bouhrim, A. Elbouzidi, H. Ouassou, L. Kharchoufa, A. Baraich, A. Atbir, F.Z. Ayyad, A. Drioiche, M. Addi, C. Hano, T. Zair, Quality Control, Phytochemical profile, and antibacterial effect of Origanum compactum Benth. Essential oil from Morocco, Int. J. Plant Biol. 13 (2022) 546–560, https://doi.org/10.3390/ijpb13040044.
[53] K. Diass, M. Merzouki, K. Elfazazi, H. Azzouzi, A. Challioui, K. Azzaoui, B. Hammouti, R. Touzani, F. Depeint, A. Ayerdi Gotor, Essential oil of Lavandula officinalis: chemical composition and antibacterial activities, Plants 12 (2023) 1571.
[54] C. Slimani, H. Sqalli, R. Chaimae, A. Farah, A. Lazraq, L. El Ghadraoui, S. Belmalha, G. Echchgadda, Chemical composition and evaluation of biological effects of essential oil and aqueous extract of Lavandula angustifolia L, Not. Sci. Biol. 14 (2022) 11172.
[55] A. Talbaoui, N. Jamaly, M. Aneb, A. Idrissi, M. Bouksaim, S. Gmouh, S. Amzazi, M. Moussaouiti, A. Benjouad, Y. Bakri, Chemical composition and antibacterial activity of essential oils from six Moroccan plants, J. Med. Plants Res. 6 (2012) 4593–4600.
[56] R. Wells, F. Truong, A.M. Adal, L.S. Sarker, S.S. Mahmoud, Lavandula essential oils: a current review of applications in medicinal, food, and cosmetic industries of lavender, Nat. Prod. Commun. 13 (2018), 1934578X1801301038.
[57] N. Chahboun, A. Esmail, H. Abed, M. Barrahi, R. Amiyare, M. Berrabeh, H. Oudda, M. Ouhssine, Evaluation de l'activité bactériostatique d'huile essentielle de la Lavandula Officinalis vis-à-vis des souches d'origine clinique résistantes aux antibiotiques, J, Materials Environ. Sci 6 (2015) 1186–1191.
[58] R.S. Verma, L.U. Rahman, C.S. Chanotiya, R.K. Verma, A. Chauhan, A. Yadav, A. Singh, A.K. Yadav, Essential oil composition of Lavandula angustifolia Mill. cultivated in the mid hills of Uttarakhand, India, J. Serb. Chem. Soc. 75 (2010) 343–348.
[59] S. Kulevanova, G. Stefkov, M. Ristić, Examination of flowers and essential oil of Lavandula officinalis grown on mountain Kozjak (Macedonia), Bull. Chem. Technol. Macedonia 19 (2000) 165–169.
[60] N. Dudareva, A. Klempien, J.K. Muhlemann, I. Kaplan, Biosynthesis, function and metabolic engineering of plant volatile organic compounds, New Phytol. 198 (2013) 16–32.
[61] N. El Hachlafi, H.N. Mrabti, S.H. Al-Mijalli, M. Jeddi, E.M. Abdallah, N. Benkhaira, H. Hadni, H. Assaggaf, A. Qasem, K.W. Goh, Antioxidant, volatile compounds; antimicrobial, anti-inflammatory, and dermatoprotective properties of Cedrus atlantica (Endl.) Manetti Ex Carriere essential oil: in vitro and in silico investigations, Molecules 28 (2023) 5913.
[62] Y.C. Martin, A bioavailability score, J. Med. Chem. 48 (2005) 3164–3170, https://doi.org/10.1021/jm0492002.
[63] I. Hubatsch, E.G.E. Ragnarsson, P. Artursson, Determination of drug permeability and prediction of drug absorption in Caco-2 monolayers, Nat. Protoc. 2 (2007) 2111–2119, https://doi.org/10.1038/nprot.2007.303.
[64] V. Urzì Brancati, C. Scarpignato, L. Minutoli, G. Pallio, Use of pharmacogenetics to optimize immunosuppressant therapy in kidney-transplanted patients, Biomedicines 10 (2022) 1798, https://doi.org/10.3390/biomedicines10081798.
[65] J. Yin, J. Wang, Renal drug transporters and their significance in drug–drug interactions, Acta Pharm. Sin. B 6 (2016) 363–373, https://doi.org/10.1016/j.apsb.2016.07.013.
[66] A. Daina, V. Zoete, A BOILED-egg to predict gastrointestinal absorption and brain penetration of small molecules, ChemMedChem 11 (2016) 1117–1121, https://doi.org/10.1002/cmdc.201600182.
[67] L. Pinzi, G. Rastelli, Molecular docking: shifting paradigms in drug discovery, Int. J. Mol. Sci. 20 (2019) 4331.
[68] T.I. Adelusi, A.-Q.K. Oyedele, I.D. Boyenle, A.T. Ogunlana, R.O. Adeyemi, C.D. Ukachi, M.O. Idris, O.T. Olaoba, I.O. Adedotun, O.E. Kolawole, Molecular modeling in drug discovery, Inform. Med. Unlocked 29 (2022) 100880.
[69] M. Attjioui, S. Ryan, A.K. Ristic, T. Higgins, O. Goñi, E.R. Gibney, J. Tierney, S. O'Connell, Comparison of edible brown algae extracts for the inhibition of intestinal carbohydrate digestive enzymes involved in glucose release from the diet, J. Nutr. Sci. 10 (2021) e5.
[70] A.A. Qurtam, H. Mechchate, I. Es-safi, M. Al-zharani, F.A. Nasr, O.M. Noman, M. Aleissa, H. Imtara, A.M. Aleissa, M. Bouhrim, A.S. Alqahtani, Citrus flavanone narirutin, in vitro and in silico mechanistic antidiabetic potential, Pharmaceutics 13 (2021), https://doi.org/10.3390/pharmaceutics13111818.
[71] H. Mechchate, I. Es-Safi, M. Bourhia, A. Kyrylchuk, A. El Moussaoui, R. Conte, R. Ullah, E. Ezzeldin, G.A. Mostafa, A. Grafov, H. Bekkari, D. Bousta, In-vivo antidiabetic activity and in-silico mode of action of LC/MS-MS identified flavonoids in oleaster leaves, Molecules 25 (2020), https://doi.org/10.3390/molecules25215073.
[72] D. Suvd, Z. Fujimoto, K. Takase, M. Matsumura, H. Mizuno, Crystal structure of Bacillus stearothermophilus a-amylase: possible factors determining the Thermostability1, J. Biochem. 129 (2001) 461–468, https://doi.org/10.1093/oxfordjournals.jbchem.a002878.
[73] N. Aghajari, R. Haser, G. Feller, C. Gerday, Crystal structures of the psychrophilic α-amylase from Alteromonas haloplanctis in its native form and complexed with an inhibitor, Protein Sci. 7 (1998) 564–572, https://doi.org/10.1002/pro.5560070304.
[74] C. Ragunath, S.G.A. Manuel, C. Kasinathan, N. Ramasubbu, Structure-function relationships in human salivary α-amylase: role of aromatic residues in a secondary binding site, Biologia 63 (2008) 1028–1034, https://doi.org/10.2478/s11756-008-0163-3.
[75] C. Ragunath, S.G.A. Manuel, V. Venkataraman, H.B.R. Sait, C. Kasinathan, N. Ramasubbu, Probing the role of aromatic residues at the secondary saccharide-binding sites of human salivary α-amylase in substrate hydrolysis and bacterial binding, J. Mol. Biol. 384 (2008) 1232–1248.
[76] O. Llorens, J.J. Perez, A. Palomer, D. Mauleon, Differential binding mode of diverse cyclooxygenase inhibitors, J. Mol. Graph. Model. 20 (2002) 359–371.

[77] L.J. Marnett, S.W. Rowlinson, D.C. Goodwin, A.S. Kalgutkar, C.A. Lanzo, Arachidonic acid oxygenation by COX-1 and COX-2: mechanisms of catalysis and inhibition* 210, J. Biol. Chem. 274 (1999) 22903–22906.
[78] V. Limongelli, M. Bonomi, L. Marinelli, F.L. Gervasio, A. Cavalli, E. Novellino, M. Parrinello, Molecular basis of cyclooxygenase enzymes (COXs) selective inhibition, Proc. Natl. Acad. Sci. USA 107 (2010) 5411–5416.
[79] K. Paul, P. Bhattacharjee, Process optimization of supercritical carbon dioxide extraction of 1, 8-cineole from small cardamom seeds by response surface methodology: in vitro antioxidant, antidiabetic and hypocholesterolemic activities of extracts, Journal of Essential Oil Bearing Plants 21 (2018) 317–329.
[80] U. Muruganathan, S. Srinivasan, Beneficial effect of carvone, a dietary monoterpene ameliorates hyperglycemia by regulating the key enzymes activities of carbohydrate metabolism in streptozotocin-induced diabetic rats, Biomed. Pharmacother. 84 (2016) 1558–1567.
[81] U. Muruganathan, S. Srinivasan, D. Indumathi, Antihyperglycemic effect of carvone: effect on the levels of glycoprotein components in streptozotocin-induced diabetic rats, Journal of Acute Disease 2 (2013) 310–315.
[82] B.M. Moukette, V.J. Ama Moor, C.P. Biapa Nya, P. Nanfack, F.T. Nzufo, M.A. Kenfack, J.Y. Ngogang, C.A. Pieme, Antioxidant and synergistic antidiabetic activities of a three-plant preparation used in Cameroon folk medicine, Int. Sch. Res. Notices 2017 (2017).
[83] M. Lončarić, I. Strelec, T. Moslavac, D. Šubarić, V. Pavić, M. Molnar, Lipoxygenase inhibition by plant extracts, Biomolecules 11 (2021) 152.
[84] C.-J. Lee, L.-G. Chen, T.-L. Chang, W.-M. Ke, Y.-F. Lo, C.-C. Wang, The correlation between skin-care effects and phytochemical contents in Lamiaceae plants, Food Chem. 124 (2011) 833–841.
[85] G. Buchbauer, Biological activities of essential oils, handbook of essential oils: science, Technology, and Applications (2010) 235–280.
[86] B.S. Jugreet, S. Suroowan, R.K. Rengasamy, M.F. Mahomoodally, Chemistry, bioactivities, mode of action and industrial applications of essential oils, Trends Food Sci. Technol. 101 (2020) 89–105.
[87] W. Dhifi, S. Bellili, S. Jazi, N. Bahloul, W. Mnif, Essential oils' chemical characterization and investigation of some biological activities: a critical review, Medicines 3 (2016) 25, https://doi.org/10.3390/medicines3040025.
[88] C.F. Carson, K.A. Hammer, T.V. Riley, Melaleuca alternifolia (tea tree) oil: a review of antimicrobial and other medicinal properties, Clin. Microbiol. Rev. 19 (2006) 50–62.